Polymer Chemistry

ROYAL SOCIETY OF CHEMISTRY

REVIEW

View Article Online
View Journal | View Issue

Cite this: *Polym. Chem.*, 2023, **14**, 7

Disulfide-containing monomers in chain-growth polymerization

Marlena Pięta, [a] Vishal B. Purohit, [a] Joanna Pietrasik [b] and Christopher M. Plummer *[a]

Due to the significance of disulfide bonds within modern material and medicinal sciences, much attention has been paid to the synthesis of disulfide-containing polymers. Within this review article, we attempt to provide a comprehensive overview of the diversity of disulfide-containing polymers that can be obtained by the chain-growth polymerization of disulfide-containing monomers. This article covers the synthesis of polymers by free radical polymerization (FRP), *i.e.*, vinyl monomers having side-chains incorporating disulfide bonds, and also the polymerization of disulfide containing heterocyclic monomers by ring-opening polymerization (ROP/rROP/ROMP). In addition, polymerization where disulfide-containing heterocycles undergo a ring-opening process that directly involves the disulfide bond are discussed. The article summarizes the state-of-the-art in polymer synthesis, and also outlines various post-polymerization modifications and biological application studies that demonstrate the importance of disulfide containing macromolecules in polymer science.

Received 10th October 2022,
Accepted 28th November 2022

DOI: 10.1039/d2py01291j

rsc.li/polymers

1. Introduction

Disulfides are generally regarded as dynamic covalent bonds and have a typical dissociation energy of *ca.* 60 kcal mol^{-1} (251 kJ mol^{-1}), far exceeding the non-covalent interactions that are present in supramolecular polymers (4–20 kJ mol^{-1}).[1] Nevertheless, disulfide bonds can be readily cleaved and replaced with other bonds, as well as reformed on demand.

[a]*International Centre for Research on Innovative Biobased Materials (ICRI-BioM)—International Research Agenda, Lodz University of Technology, Zeromskiego 116, 90-924 Lodz, Poland. E-mail: christopher.plummer@p.lodz.pl*
[b]*Institute of Polymer and Dye Technology, Faculty of Chemistry, Lodz University of Technology, Zeromskiego 116, 90-924 Lodz, Poland*

Marlena Pięta

Marlena Pięta completed her Ph.D. in 2018 at Lodz University of Technology (TUL), Poland in the area of organic synthesis, specifically the synthesis of chiral aza-heterocycles with cytotoxic activity. In 2019 she worked as researcher in the process chemistry department in Ryvu Therapeutics, Poland. Since 2020 she has been employed as a post-doctorate at TUL. In 2020–2021 she worked on the synthesis of biologically active compounds and profluorescent probes for ROS in a medicinal chemistry group, and from 2022 onwards she is working on the synthesis of new monomers for radical ring-opening polymerization (rROP) in a polymer chemistry group.

Vishal B. Purohit

Vishal Purohit completed his Ph.D. in 2017 under the supervision of Dr K. H. Patel and Prof. D. K. Raval at S. P. University (India), where he studied NHC-transition metal catalyzed C–H activation reactions. Between 2017–2020 he was employed as an Assistant Professor at Shri A. N. Patel PG Institute of Science and Research (India). During 2020–2021, he worked as a Postdoc with Prof. Karol Grela at the University of Warsaw (Poland). In November 2021, he joined the group of Dr Christopher Plummer as a Postdoc at Lodz University of Technology (Poland), working on the synthesis of new monomers for ring-opening polymerization.

The range of potential cleaving and bond exchanging triggers is extensive, with multiple physical (*e.g.* light, heat, mechanical force, magnetic field) and chemical triggers (*e.g.* nucleophiles, reducing agents, radicals). In nature, disulfide bonds occur in abundance as part of the intramolecular cross-linking of peptides and protein backbones. Indeed, the stability of such naturally occurring macromolecules relies upon the participation of disulfide bonds within their secondary and tertiary structures (*e.g.* α-helix), these structures being essential for physiological activity (Fig. 1A).[2] Cysteine-derived disulfide cross-linking is present in proteins of various sizes and functions, from small (10–50 amino acid) peptides such as growth factors and cytokines, to cysteine-rich biomaterials such as keratin-associated proteins and other supramolecular assemblies. Although disulfide linkages are plentiful in cysteine-rich materials, they are also important for the stabilization of surface loops and secondary structure domains that are vital for the physiological activity of proteins (Fig. 1B). Moreover, there also exists many naturally occurring non-peptide disulfides, for example the enzyme cofactor essential for aerobic metabolism α-lipoic acid **M1**, and asparagusic acid **M2** which can be isolated from *Asparagus officinalis*,[3] among others[4,5] (Fig. 1C).

The incorporation of disulfide bonds into a polymer backbone can instil polymers with properties that include adhesion, flexural strength, adaptability, degradability, and even self-repair.[6] Pendent disulfide functionalities can be exploited to prepare polymers with stimuli-sensitive and dynamic architectures. The reversible polymerization of cyclic disulfides, in particular 1,2-dithiolanes, has been widely exploited in bioconjugation and the design of self-healing materials.[7–9] Moreover, polymers displaying disulfide-containing pendant groups demonstrate significant stability in the blood stream and the extracellular environment, while simultaneously displaying reactivity to intracellular antioxidants

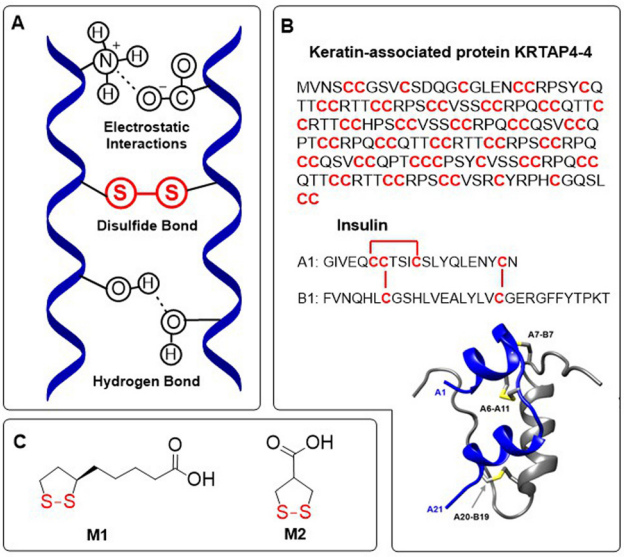

Fig. 1 (A) Disulfide cross-linking in proteins influences the formation of secondary and tertiary structures; (B) keratin-associated protein KRTAP4-4 represents a disulfide-rich protein with cysteine constituting 37% of the amino acid sequences, and peptide hormone insulin which consists of two chains bound together by disulfide bonds. Ribbon diagram of insulin showing the location of disulfide bonds, adapted under a Creative Commons licence from van Lierop *et al.*;[11] (C) naturally occurring 1,2-dithiolanes.

such as glutathione (GSH). This phenomenon has been widely exploited for the transportation of therapeutic agents attached *via* disulfide bond to the intracellular environment, readily enabling the circumvention of innate obstacles (*e.g.* lipophilicity).[10]

Due to the significance of disulfide bonds in modern polymer chemistry, we present this review article focusing on disulfide-containing polymers synthesized by chain-growth

Joanna Pietrasik

Joanna Pietrasik received her Ph.D. in 2003 at Lodz University of Technology (TUL), Poland; next she spent 2 years at Carnegie Mellon University (CMU), USA, in the group of Prof. Matyjaszewski as a postdoc. She obtained her habilitation degree in 2014. She now holds the position of professor at TUL. Her research activity is dedicated to polymer synthesis, inorganic particles, surface modifications, as well as hybrid materials and nanocomposite properties.

Christopher M. Plummer

Christopher Plummer completed his Ph.D. in 2016 at RMIT University, Australia in the area of organic synthesis, specifically the synthesis of oxygenated heterocycles. Between 2016–2019 he was employed as a post-doctorate at Sun Yat-sen University (SYSU), China working on the post-modification of polyolefins. In 2019–2021 he worked as a researcher in an industry-funded position at Aix-Marseille University, France, working on the synthesis of new monomers for radical ring-opening polymerization (rROP). Following this, he took up a position as Junior Principal Investigator at Lodz University of Technology (TUL), Poland, and is a presently a group leader in polymer chemistry.

polymerization. The article encompasses disulfides located within both the polymer backbone and the pendant side-chains, specifically those that originate from disulfide-containing monomers. The article is divided into multiple sections. Within the first section the synthesis of polymers by free-radical polymerization (FRP) is reviewed, *i.e.*, vinyl monomers that have side-chains incorporating disulfide bonds. Then, the synthesis of polymers using disulfide-containing cyclic monomers by ring-opening polymerization (rROP/ROP/ROMP) is reviewed. Within these sections, interesting post-modifications, assembly formations and biological studies will be discussed which additionally support and substantiate research at the synthetic level. Following this, polymerization where disulfide-containing monomers undergo a ring-opening process involving the disulfide bond are covered. Finally, a section describing common methods for monomer synthesis is included. The scope of the article is limited to the polymerization of disulfide-containing monomers, and therefore trisulfide-containing monomers and the vulcanization of rubber are outside of the scope and are not covered.

2. Free-radical polymerization

During the process of free-radical polymerization (FRP) a polymer is formed by the successive addition of monomers to an actively propagating radical-containing chain end. In a typical polymerization, an initiator commences the polymerization by its homolytic degradation to form a radical species which then adds to the radical-acceptor moiety (alkene, alkyne, thiocarbonyl, *etc.*) of a monomer. This mechanistic process generates a new radical, and the propagation process repeats until radical termination. As the propagating chains are all initiated at different times, this leads to non-homogenous polymer samples. As specialist polymer applications require more precisely controlled polymer architectures, various techniques known under the umbrella term "reversible-deactivation radical polymerization" (RDRP) can be applied. In an ideal RDRP process, the molecular weight of the growing polymer chains increases equally with time. The most prominent RDRP techniques are atom transfer radical polymerization (ATRP), reversible addition/fragmentation chain transfer polymerization (RAFT), and nitroxide-mediated polymerization (NMP).

2.1 Monomers containing pendant disulfide functionality

The incorporation of disulfide bonds into pendant side-chains of a polymer allows for the fine adjustment of polymer properties by enabling post-polymerization modification. Typical post-modifications include thiol-disulfide exchange with thiolated molecules, reduction followed by utilization of the free thiol group as a nucleophile, and polymer gelation by disulfide bond metathesis. Polymers containing pendant disulfide bonds have therefore attracted attention for the design of targeted drug delivery systems. Selective activation and payload release is enabled by the disulfide group, being tuned to characteristics such as acidity or antioxidant concentration. Thus, in recent years there have been a multitude of reports detailing polymer micelles with covalently linked or encapsulated anti-tumour agents. In this section, polymers synthesized from (2.1.1) pyridyl disulfide monomers, (2.1.2) monomers with disulfide self-immolative linkers, and (2.1.3) bifunctional cross-linking agents are presented.

2.1.1 Pyridyl disulfide monomers. The incorporation of the pyridyl disulfide group into a polymer enables facile thiol–disulfide exchange which provides ready access to post-modification (Fig. 2A).[12] During the exchange process a 2-pyridinethione leaving group is released, which is stable and unreactive. The primary tautomeric form of 2-pyridinethione is the thioketone and therefore it cannot be involved in further exchange reactions which thereby provides a driving force to shift the equilibrium towards quantitative post-modification. Furthermore, these disulfide exchanges can be performed in both aqueous and organic media under mild conditions, with good yields and wide functional group tolerance. In addition, analysis by UV-Vis spectroscopy enables the convenient tracking of reaction progress (*e.g.* 2-pyridinethione λ_{max} = 375 nm; pyridyl disulfide λ_{max} = 280 nm).[13] An additional benefit of the pyridyl disulfide is their lipophilicity which can be used to contribute to supramolecular assembly in the aqueous phase, and for closing lipophilic molecules within the hydrophobic core. Monomers bearing pyridyl disulfide functionality are presented in Fig. 2B. Acrylate analogues **M3** (PDEA) and **M7** (PDPA) and methacrylate **M5** (PDEM) are the most reported, followed by (meth)acrylamides **M4** (PDEAA) and **M6** (PDEMA).

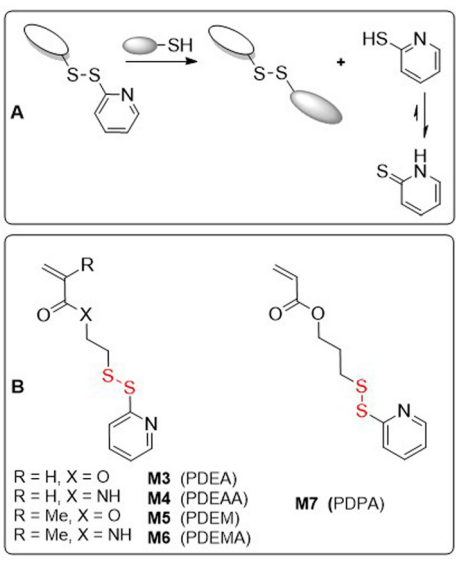

Fig. 2 (A) Application of pyridyl disulfide group in a thiol–disulfide exchange giving a new disulfide and unreactive 2-pyridinethione; (B) monomers containing pyridyl disulfide groups.

Monomers containing pyridyl disulfide moieties have been demonstrated to be useful in a range of modern polymer synthesis techniques, including FRP, ATRP and RAFT. In 1998, Ruffner and coworkers, desiring to obtain a polymer with functional pendant groups that were stable under aqueous conditions, copolymerized methacrylamide **M6** with *N*-(2-hydroxypropyl)methacrylamide (**HPMA**) to fabricate polymers with up to 8.3 mol% **M6**.[13] The authors confirmed that the pyridyl disulfide group was stable in aqueous media at pH ≤8, as well as capable of undergoing rapid thiol–disulfide exchange with L-cysteine or 2-mercaptoethanol in aqueous solution. **Poly(HPMA-*co*-M6)** was also conjugated with thiol-modified oligonucleotides and effectively absorbed into HeLa cells *via* endocytosis.

Hoffman and coworkers later copolymerized **M7** with butyl acrylate (**BA**) and methacrylic acid (**MAA**) to produce amphiphilic random terpolymers with up to 7 mol% **M7** and M_n values of 10.6–124 kg mol^{-1} ($Đ$ = 1.3–2.3).[14] These polymers were readily conjugated with oligopeptides by disulfide bond, and complexed with therapeutic nucleic acids. It was confirmed that **poly(M7-*co*-BA-*co*-MAA)** readily diffused into the cell cytoplasm where it exhibited low cell toxicity. Moreover, it was also demonstrated that disulfide-conjugated drugs can be released in the presence of GSH. Alternative polymers where **MAA** was replaced with pH sensitive monomers such as ethylacrylic acid (**EAA**) or propylacrylic acid (**PAA**) were also reported.[15]

Thayumanavan and coworkers applied RAFT and ATRP techniques for the fabrication of copolymers of **M5** and *N*-hydroxysuccinimide methacrylate (**NHSMA**).[16] Homopolymerization of **M5** under RAFT conditions resulted in an insoluble product. Fortunately, an ATRP-based approach successfully provided **polyM5** with an M_n = 6.7 kg mol^{-1} ($Đ$ = 1.2). Under analogous conditions, **poly(NHSMA-*co*-M5)** were obtained with M_n values of 9.7–19.0 kg mol^{-1} ($Đ$ = 1.3–1.6). Finally, thiol–disulfide exchange reactions using 1-undecanethiol and thiol-modified fluorescent anthracene were performed to study their release profiles using the reducing agent 1,4-dithiothreitol (DTT).

Bulmus and coworkers synthesized **polyM5** using RAFT and then subjected it to thiol–disulfide exchange with 3-mercaptopropionic acid, 4-mercaptobutanol, 11-mercaptoundecanol, and reduced L-glutathione (GLT). The obtained modified polymers subsequently self-assembled into spherical nanoparticles in aqueous solution.[17] **PolyM5** was also applied as a macro-RAFT agent for the polymerization of **HPMA** to provide amphiphilic block copolymers (Fig. 3).[18] Treatment of these block polymers with tris(2-carboxyethyl)phosphine (TCEP) led to successful conjugation with maleimide-modified anticancer drug doxorubicin (DOX), with simultaneous cross-linking and self-assembly. The formed nanomicelles were reported to exhibit *in vivo* stability and released the conjugated DOX at acidic pH.

Later, Thayumanavan and coworkers presented multiple research articles concerning polymers with incorporated pyridyl disulfide moieties.[19–32] For example, RAFT copolymerization of **M5** and poly(ethylene oxide) monomethacrylate (**PEGMA**) provided **poly(M5-*co*-PEGMA)** which was used to

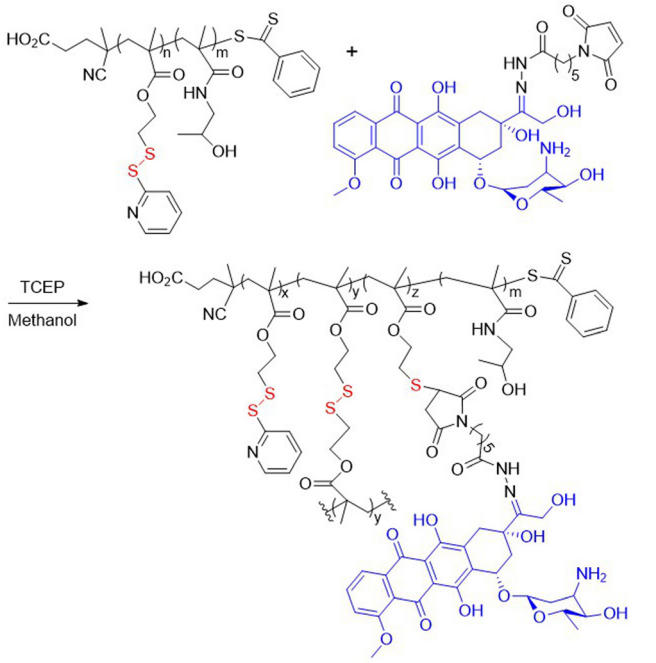

Fig. 3 Conjugation of poly(M5-*b*-HPMA) with maleimide-modified DOX with simultaneous cross-linking.

generate well-defined spherical nanogels by its treatment with DTT, with the size dependent on both the monomer ratio and the presence of various salts.[19,20,23] Subsequently, the formation of micelles with encapsulated hydrophobic fluorescent dyes and their release profile were studied.[19–21] In addition, it was reported that through thiol–disulfide exchange **poly(M5-*co*-PEGMA)** could be equipped with protein ligands that could facilitate receptor-dependant cell internalization.[22,24,26] Conjugates of **poly(M5-*co*-PEGMA)** and caspase-3 proteins were reported able to enter HeLa cell lines, unlike the unconjugated protein.[30] Post-modification in which pyridyl disulfide groups were exchanged with various small-molecules provided multi-stimuli-responsive polymers that were reactive to chemical (redox, pH), biological (protein) and/or physical (light) stimuli.[25]

Additionally, thiol–disulfide exchange of **poly(M5-*co*-PEGMA)** with 2-mercaptoethanol followed by condensation of the resulting alcohol with 4-nitrophenyl chloroformate provided modified polymer containing *p*-(nitrophenylcarbonate) ethyl disulfide pendants (Fig. 4A). These alternative disulfide-containing pendant groups were reported to be less sterically hindered than pyridyl disulfide groups and therefore allowed for accelerated GSH-induced payload release.[31] These polymers were then conjugated with lysine-containing proteins and diamine cross-linkers using amine-carbonate condensation. **Poly(M5-*co*-PEGMA)** was also subjected to methylation of the pyridyl nitrogen, with the resulting cationic groups readily undergoing complexation with nucleic acids *via* electrostatic interactions (Fig. 4B).[32] Following subsequent cross-linking, these fabricated nanoassemblies were reported to exhibit lower

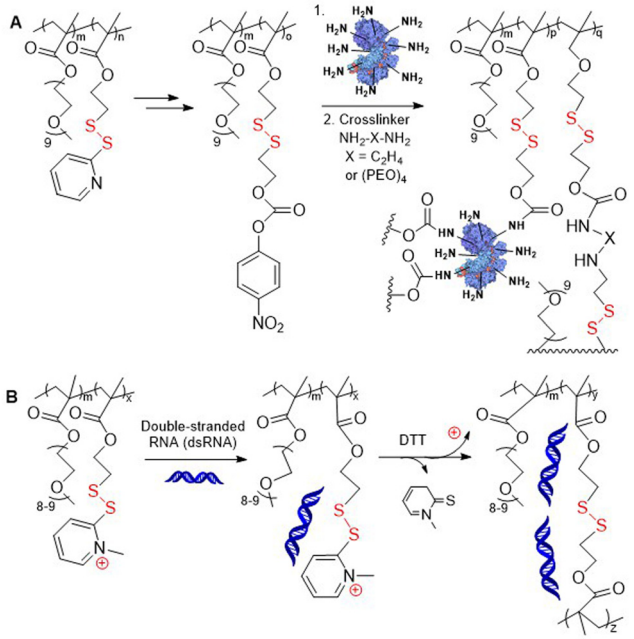

Fig. 4 (A) Post-modification of poly(PEGMA-*co*-M5) for protein conjugation; (B) complexation of poly(PEGMA-*co*-MeM5) with dsRNA through electrostatic interaction.

cytotoxicity compared to classical delivery vehicles, which was attributed to their non-cationic character.

Terpolymers obtained by the RAFT copolymerization of **M5**, **PEGMA** and 2-(diisopropylamino) ethyl methacrylate (**DPAM**) were converted into nanogels in an aqueous solution of DTT.[27,28] The introduction of diisopropylamine moieties was intended to enable the nanogel to be positively charged at an acidic pH to assist in cellular uptake. In addition, the RAFT copolymerization of **M5**, **PEGMA** and glycidyl methacrylate (**GMA**) provided a polymer which was used to form and study composite supramolecular nanoassemblies.[29] **Poly(PAA-*b*-DMA-*co*-M6)** (DMA = *N*,*N*-dimethylacrylamide) obtained by RAFT polymerization was conjugated to ovalbumin which had been modified by the introduction of a thiol moiety.[33] The conjugates were tested as protein-based vaccines and were reportedly able to stimulate the immune system of mice, and to subsequently enhance the rejection of cancer cells.

Xu and coworkers explored **M3**-based polymers obtained by FRP.[34–41] Thus, **polyM3**, **poly(M3-*co*-PEGMA)** and **poly(M3-*co*-PEGMA-*b*-NiPMA)** (NiPMA = *N*-isopropylmethacrylamide) were fabricated, with the pyridyl disulfide groups then subjected to post-modification, being replaced with various active molecules including camptothecin (CPT),[36] Herceptin,[36] acetylcysteine,[40] diethyldithiocarbamate,[41] disulfiram,[42] and lactobionic acid.[38,41] Some of the modified polymers were also subjected to aqueous self-assembly to give micelles encapsulating anticancer agents such as paclitaxel,[34] doxorubicin[34,35] or a silicon photosensitiser for photodynamic therapy.[37] **Poly(M3-*co*-PEGMA)** was also obtained by RAFT methodology (M_n = 7.8 kg mol^{-1}, $Đ$ = 1.27) and subjected to nanogel formation in the presence of DTT to encapsulate DOX.[42]

In 2012, Jackson and Fulton copolymerized **M4** with *N*-ethylacrylamide-2-(4-formylbenzamide) (**EFB**) or *N*-(*tert*-butoxycarbonyl)-propylaminoacrylamide (**PAAA**) to provide **poly(M4-*co*-EFB-*co*-DMA)** and **poly(M4-*co*-PAAA-*co*-DMA)** *via* RAFT methodology.[43] After removal of the Boc protection, both polymers were cross-linked through imine bond formation. Additionally, during this process a hydrophobic dye was encapsulated. The nanoassembly was further strengthen by disulfide linkage formation resulting from its treatment with DTT. It was reported that the release of the dye readily occurred in the presence of a reducing agent at lowered pH. Similarly, **poly(M4-*co*-EFB-*co*-DMA)** was obtained by Segura-Sánchez *et al.* and was linked with thiolated chitosan by both imine and disulfide linkage, with acidic and reductive conditions allowing chitosan cleavage.[44] Ji and coworkers copolymerized 2-methylene-1,3-dioxepane (**MDO**) with **PEGMA** and **M5** to provide a terpolymer with an M_n = 24.0 kg mol^{-1} ($Đ$ = 1.58) (Fig. 5).[45,46] The **poly(MDO-*co*-PEGMA-*co*-M5)** was subsequently grafted with DOX and then self-assembled to provide spherical micelles which exhibited strong toxicity against lung carcinoma cells, while blank micelles reported to be non-toxic.

In addition, DOX was encapsulated into a pseudo-diblock polymer of **M5** and hyaluronic acid (HA), obtained *via* ATRP methodology with a subsequent azide click-reaction, which was then self-assembled into micelles and subsequently cross-linked.[47] The system exhibited excellent bloodstream stability and high tumor targeting, as well as improved therapeutic efficacy. In addition, RAFT polymerization was utilized to synthesize **poly(M6-*co*-HPMA)** with an M_n = 13.0 kg mol^{-1} ($Đ$ = 1.13) (Fig. 6).[48] This macro-chain transfer agent (macro-CTA) was subsequently copolymerized with **HPMA** and a methacrylamide-functionalized oligolysine monomer, followed by conjugation with an endosomolytic peptide, melittin. The resulting block copolymer was then electrostatically complexed with plasmid DNA to provide a gene delivery system that exhibited enhanced delivery to both HeLa and neuron-like cell lines.

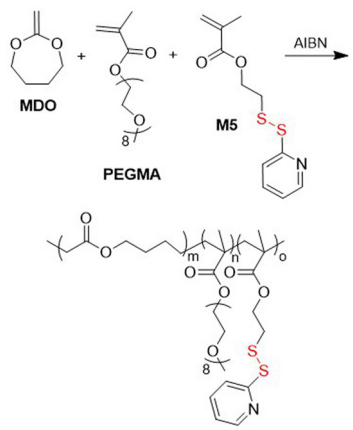

Fig. 5 Synthesis of poly(MDO-*co*-PEGMA-*co*-M5).

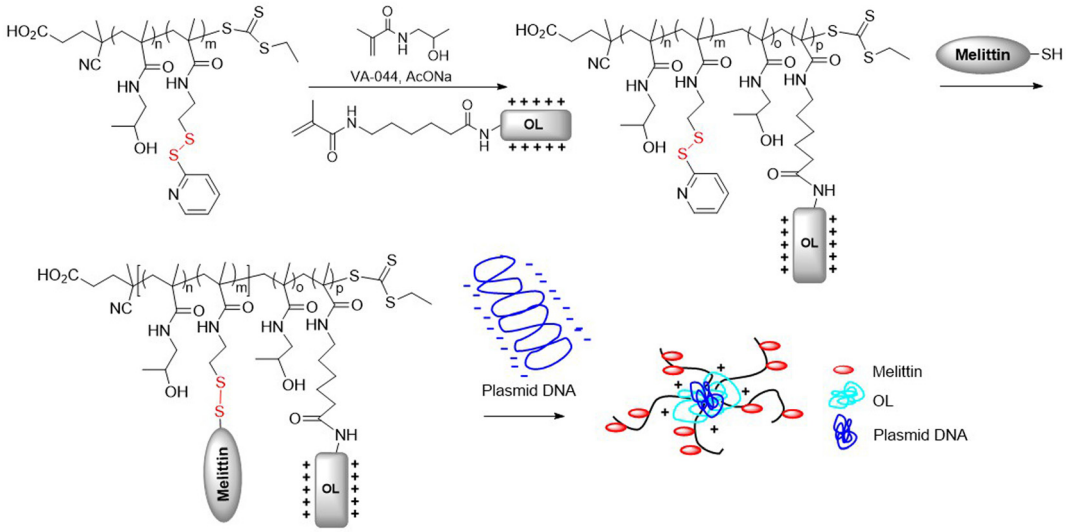

Fig. 6 Gene delivery system of polymer with oligolysine (OL), melittin and plasmid DNA.

Water soluble **poly(NiPAA-*co*-AA-*co*-M4)** with an M_n = 100 kg mol^{-1} ($Đ$ = 5.1) was conjugated with thiolated single strand DNA, and by subsequent hybridization with the complementary DNA strand, a double strand DNA conjugate was formed which was then applied for aggregation studies.[49] **Poly(M5-*b*-PEG)** (PEG = polyethylene glycol) obtained by RAFT polymerization with an M_n = 11.6 kg mol^{-1} was stirred with gold nanoparticles in DMF to provide polymer-coated AuNPs with a virtually neutral surface which exhibited good stability under various physiological conditions and reduced non-specific adsorption of biomolecules.[50] Oxopentanoate ethyl methacrylate (**OPM**) and a pyrene-terminated RAFT agent were utilized in synthesis of tri-block terpolymer **poly(OPM-*b*-M3-*b*-PEG)** (Fig. 7).[51] This macromolecule was conjugated with *O*-benzylhydroxylamine (BHA) *via* imine bond formation with the ketone group of **OPM**. Then, the modified polymer was attached to graphene through π–π stacking interactions resulting in a polymer/graphene composite, with BHA and 2-pyridinethione (PT) release being investigated.

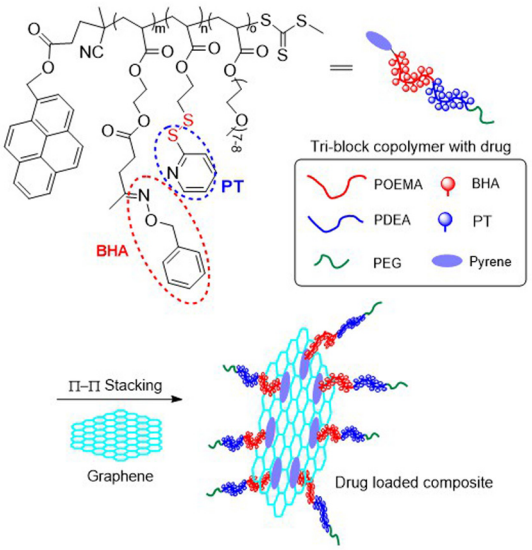

Fig. 7 Synthesis of polymer/graphene composite from poly(OPM-*b*-M3-*b*-PEG).

Applying RAFT polymerization, **M6** was incorporated into **poly(MCT-*co*-M6-*b*-PEGMA-*co*-DEM)**, where **MCT** equals "methacrylated macrocyclic coumarin caged thiol" (Fig. 8A/B).[52] An aqueous solution of this polymer was then cross-linked by light irradiation to produce nanoparticles that were able to encapsulate hydrophobic compounds. These nanoparticles were reported to exhibit good stability, performing the controlled release of guest molecules under redox conditions. The mechanism of the photo-triggered cross-linking initiates with the release of free thiol from the photo-responsive MCT moiety which subsequently reacts with pyridyl disulfide functional groups to create disulfide bridges (Fig. 8C).[53] By the application of various irradiation conditions, different cross-linking densities were accomplished.

A series of statistical copolymers involving **M5** and *N*-vinyllactams were prepared *via* RAFT methodology.[54] The authors fabricated polymer film by spin-coating a solution of **poly(NVP-*co*-M5)** (**NVP** = *N*-vinylpyrrolidone) on solid substrates, which was then functionalized by treatment with an aqueous solution of thiol-containing molecules. It was demonstrated that these films promoted the adhesion and growth of HeLa cell lines, unlike PEG-based polymers. A number of potential copolymer carriers possessing an incorporated pyridyl disulfide moiety were also obtained by RAFT methodologies. Terpolymer **poly(PEGMA-*co*-PDEGMA-*co*-M5)** was synthesized and then conjugated with thiol-functionalized porcine pancreatic lipase to produce thermo-responsive nanogels upon treatment with a meso-2,3-dimercaptosuccinic acid (DMSA) solution.[55] Similarly, **poly(tBMA-*co*-M5)** (TBM = *tert*-

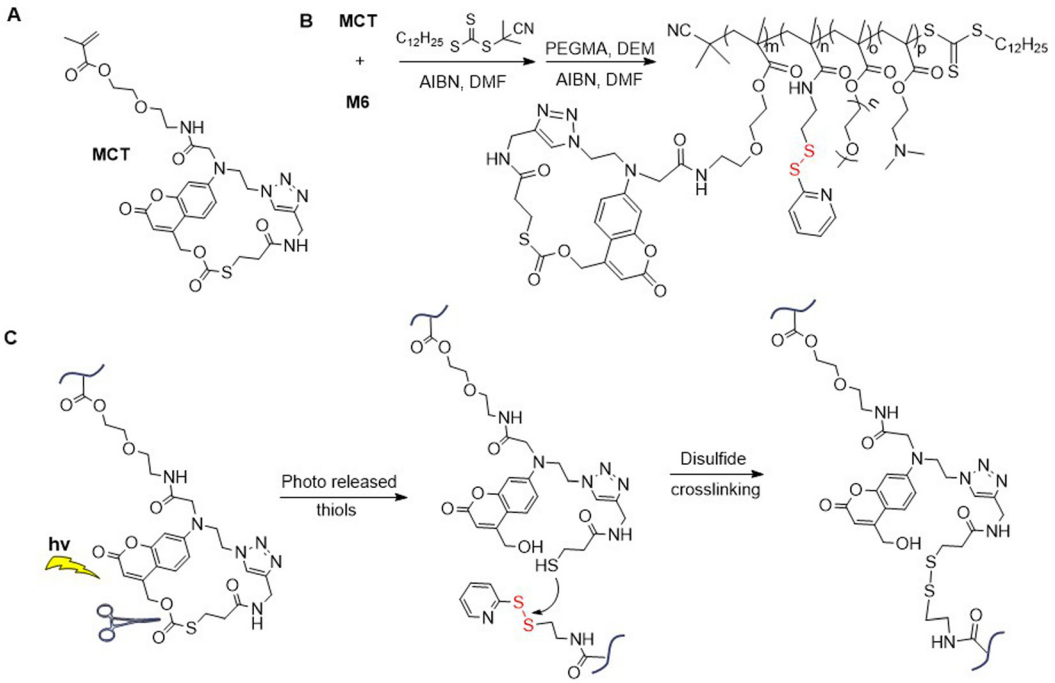

Fig. 8 (A) Structure of MCT; (B) synthesis of poly(MCT-*co*-M6-*co*-PEG-*co*-DEM); (C) photo-triggered cross-linking of poly(MCT-*co*-M6-*co*-PEGMA-*co*-DEM).

butylmethacrylate) was conjugated to bovine serum albumin (BSA) to provide covalently connected nanostructures.[56] In another study, **poly(PDEGMA-*b*-(PEGMA-*co*-M5))** was self-assembled above its lower critical solution temperature (LCST) and then cross-linked with reduced BSA.[57] After lowering the temperature to below the LCST, proteinosomes containing preserved BSA secondary structure and activity were formed that were capable of internalization into breast cancer cell lines. In addition, **poly(DEGMA-*co*-M5)** was coupled with thiol-modified lysozyme to study the cloud point of self-assembled nanostructures, and **poly(TEGMA-*co*-M5)** was grafted with various peptides, *i.e.* bivalirudin, a thrombin inhibitor with the ability to reduce scar formation.[58,59]

2.1.2 Disulfide-containing self-immolative linkers (DSILs). Disulfide self-immolative linkers (DSILs) have received considerable attention as a strategy for the selective release of bioactive agents for therapeutic and diagnostic applications (Fig. 9).[60] This approach relies on disparities in GSH concentrations in the blood (2–10 μM) and cytosol (1–10 mM),[61] as well as disparities between cancerous and regular cells (elevated levels in the latter). Furthermore, when the disulfide moiety is part of an extended linker it serves to overcome the problem of steric hindrance for thiol attack. Moreover, this method enables the release of pristine active molecules by taking advantage of the wider scope of functional groups that can be utilized. Thus, after reductive dissociation of the disulfide bond, subsequent reshuffling of the remaining linker occurs which leads to sulfide side-product formation and subsequent release of the intact functional molecule. Self-immolative fragmentation can proceed through 1,4- or 1,6-elimination to release a quinone–methide moiety, or through intramolecular cyclization to discharge thioethers, thiolactones or thiocarbonates. For systems involving polymer carriers, mostly β-dithioethyl (β-DTE) carbamate linkers were utilized (Fig. 9). In this case, thiol group attack on the disulfide moiety results in the release of a 5-membered thiocarbonate. Interestingly, to date there have been no studies relating to the biological toxicity of this small-molecule by-product.

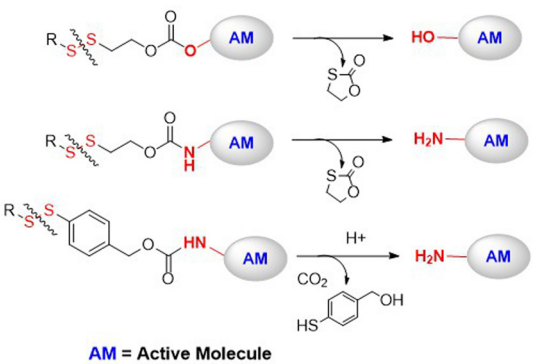

Fig. 9 DSILs that were conjugated with polymer carriers. AM = active molecule.

There are a few examples of polymer-conjugates with DSILs obtained *via* chain-growth polymerization utilizing disulfide-containing monomers. Zelikin and co-workers developed a list of macromolecular prodrugs consisting of DSILs linked to anti-

viral agents.[62–71] Monomers were prepared containing: (a) acrylate or methacrylate, (b) β-DTE carbamate linkers, and (c) bioactive molecules bound through a hydroxyl group (Fig. 10A). Activated monomers were copolymerized by RAFT with **HPMA** or **MAA**, with the authors reporting that no degradation of the disulfide bonds was observed during this process.[62] Panobinostat (PANO) possessing a secondary amine was also incorporated into a RAFT-derived copolymer (Fig. 10B).[66] Despite the low yields of the polymerization, polymers with a PANO content up to 11 mol% were obtained. Macromolecular prodrugs of ribavirin (RBV) and azidothymidine (AZT) were also obtained, being installed to levels of up to 24% by weight.[62,63,65]

All of the reported studies demonstrated a significant advantage for the use of DSILs *versus* the direct conjugation of the prodrug *via* ester linkage. Anti-inflammatory activity of RBV prodrugs in cultured macrophages showed a high dependence on both the M_n value and the drug loading percentage.[63] To address the problem of HIV drug resistance, polymers containing multiple prodrugs that were active toward numerous viral replication stages were prepared.[67,70,72] A terpolymer was thereby fabricated from **HPMA** and two methacrylate based DSILs, equipped with AZT and lamivudine (3TC) that proved to be stable under extracellular conditions, while readily releasing payloads in environments resembling the cytosol.[70,72] Moreover, this polymer exhibited synergistic potency which exceeded the unmodified prodrugs. Since polyanionic side chains are known to increase anti-HIV efficacy, the authors designed statistical copolymers equipped with sulfonate groups. Terpolymers were prepared through the RAFT copolymerization of the DSIL derivative of 3TC with *N*-hydroxyethyl acrylamide (**HEAm**) and 2-acrylamido-2-methanepropane sodium sulfonate (**AMPS**) (Fig. 10C).[67] These polymers demonstrated potent reverse transcriptase inhibition, and therefore alternative monomers containing anionic functionalities were copolymerized with ribavirine acrylate and methacrylate DSIL monomers.[69]

In 2018, Zelikin and coworkers reported albumin–polymer drug conjugates.[69–71] Terpolymers consisting of **HPMA** and AZT/3TC-methacrylate DSIL monomers were obtained with M_n values ranging from 15.9–20.3 kg mol^{-1} and a drug content of approximately 10 mol%. The polymers were then conjugated with albumin to install *ca.* 1 protein per polymer chain. It was confirmed that these conjugates provided human T cells with strong protection from HIV infection (Fig. 11A).[70] Then, a novel RAFT agent was applied for the copolymerization of **HPMA** and Acyclovir (ACV) bound through a DSIL to methacrylate, which was then non-covalently associated with albumin (Fig. 11B).[71] While the pristine drugs exhibit poor pharmacokinetics, the conjugate displayed high activity against herpes simplex virus type 2 in using mice studies.

Oupický *et al.* reported a **HPMA**-based polymeric prodrug of AMD3465 (a potent HIV entry inhibitor) bound *via* a β-DTE carbamate linker to methacrylate.[73] Radical copolymerization provided a polymer with an AMD3465 content of *ca.* 22 wt%, which could be effectively released after treatment with GSH. Moreover, due to their cationic character, these polymers were able to form nanosized polyplexes with microRNA and then to deliver it into cells. This dual-function polymer exhibited a stronger inhibition of cancer cell migration in comparison to individual treatments. In addition, camptothecin was bound *via* DSIL linkage to methacrylate and then subjected to RAFT polymerization with 2-(2-methoxyethoxy)ethyl methacrylate (**MEO$_2$MA**) in the presence of PEG$_{113}$-CPDB (CPDB = 4-(4-cyanopentanoic acid) dithiobenzoate).[74] The resulting macro-CTA was reacted with benzyl methacrylate (**BzMA**) and bis(methacryloyl)cysteamine (**BMCy**) in a RAFT polymerization, with subsequent self-assembly (Fig. 12). Diffusion of GSH molecules

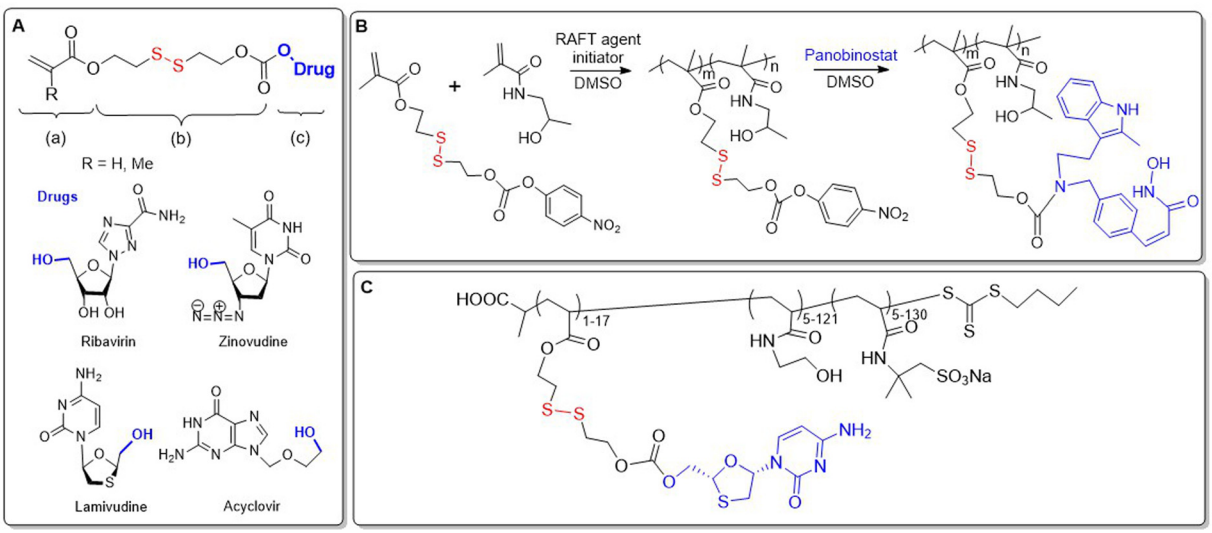

Fig. 10 (A) Macromolecular prodrug consisting of DSILs linked to antiviral agents; (B) synthesis of polymer loaded with PANO; (C) terpolymer equipped with 3TC and sodium sulfonate moieties.

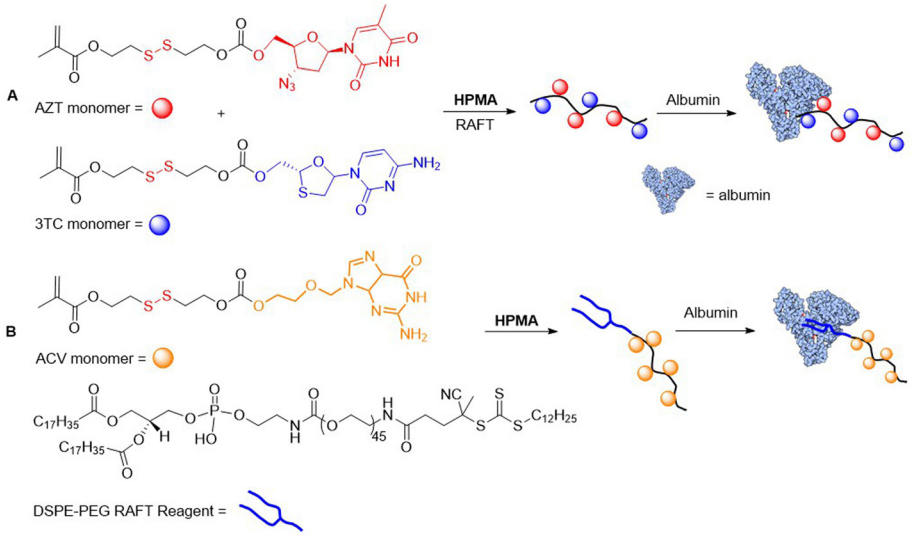

Fig. 11 (A) Synthesis of covalently bound albumin–HPMA-based polymer containing AZT/3TC-methacrylate DSILs; (B) synthesis of HPMA-based polymer–ACV conjugates which are non-covalently associated with albumin.

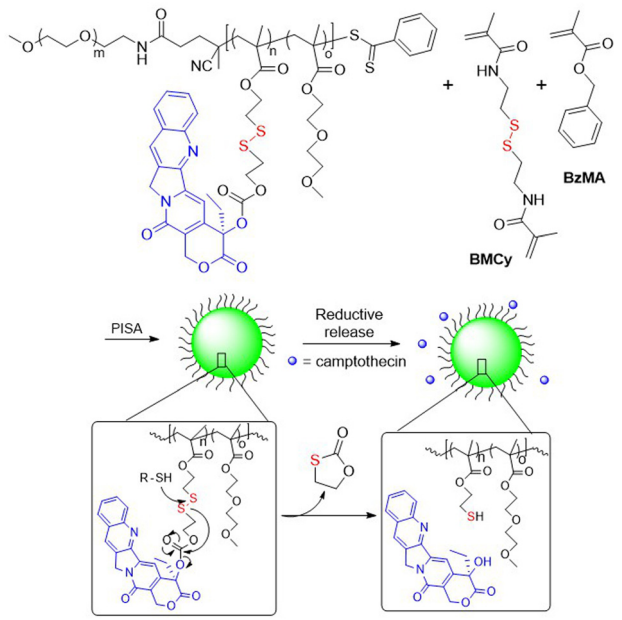

Fig. 12 Synthesis of DSIL camptothecin delivery system using RAFT polymerization, with self-assembly and reductive drug release.

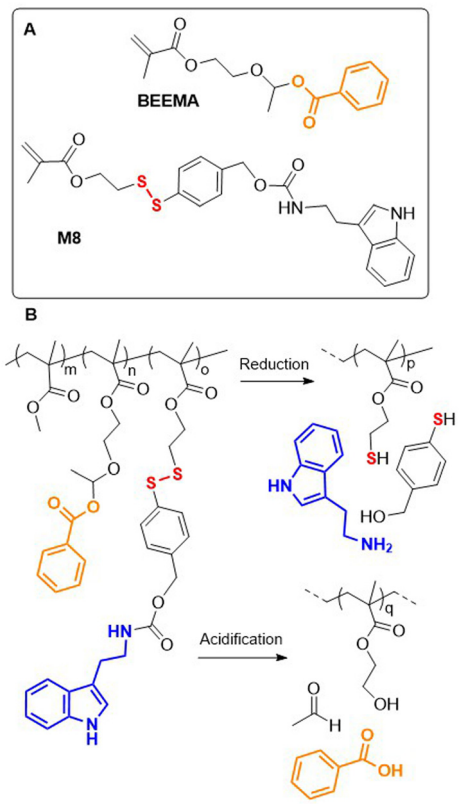

Fig. 13 (A) Monomers for synthesis of anti-corrosion coatings; (B) release of benzoic acid or tryptamine from poly(MMA-*co*-BEEMA-*co*-M8) in acidic or reductive conditions.

into the core of the nanoparticle enabled degradation of disulfide linkages, followed by reshuffling and camptothecin release.

Recently, a redox-responsive monomer **M8** was reported that displayed robust conversion *via* 1,6-elimination to release 4-mercaptobenzyl alcohol (Fig. 13A).[75] Copolymerization of **M8**, **MMA** and pH-responsive monomer **BEEMA** yielded a terpolymer that could release two corrosion inhibitors in acidic (benzoic acid) or reductive (tryptamine) conditions (Fig. 13B). The corrosion rate of steel coated with **poly(MMA-*co*-BEEMA-*co*-M8)** was reduced 800 times when compared to uncoated steel, and 19 times compared to steel coated with **poly(MMA)**.

2.1.3 Other monomers containing pendant disulfides. A series of amphiphilic copolymers were obtained from hydro-

philic tri(ethylene glycol)methyl ether acrylate and lipophilic monomer **M9**, with M_n values from 9.3–11.0 kg mol^{-1} ($Đ$ = 1.9–2.3) (Fig. 14).[76] In aqueous solution, micelle-like nanoassemblies were formed which were able to encapsulate hydrophobic dyes and drugs (*e.g.*, DOX, ≥14% w/w) and then subsequently release the payload in an aqueous GSH solution. Furthermore, an amphiphilic block copolymer was prepared from hydrophobic block of **M10** and a hydrophilic block of **PEG** *via* ATRP methodology.[77] In aqueous solution, monomodal micellar assemblies were formed, which after treatment with DTT underwent core-cross-linking or degradation, dependent upon the concentration.

2.2 Disulfide-based cross-linking monomers

An additional class of monomers that possess disulfide bonds in the pendant are the bifunctional vinyl monomers used for their cross-linking ability (Fig. 15A). Among these monomers are 2,2′-dithioethanol derivatives: acrylate **M11** (DSDA) and methacrylate **M13** (DSDMA) and cystamine derivatives: **M12** (BACy) and **M14** (BMCy) (Fig. 15B). There are reports of the utilization of ATRP and RAFT to synthesize degradable polymers with **M11** or **M13**, focusing on conditions that enable or prevent gelation. This research relies heavily on the application of the Flory–Stockmayer theory which predicts gelation based upon the quantity of cross-linking per polymer chain. The studies refer also to the synthesis of various soluble branched copolymers where monovinyl monomers were polymerized with multivinyl cross-linkers in solution,[78] emulsion,[79] or suspension,[80] and also by controlled radical cross-linking copolymerization.[81] Other reports detail the development of branched stimuli-responsive drug delivery systems that are readily degradable under intracellular reducing conditions, where monomers **M12** or **M14** are typically utilized.

Matyjaszewski and coworkers applied **M13** for the preparation of well-defined degradable copolymers by ATRP.[7,82–90] Through copolymerization of **MMA** with **M13** degradable gels were prepared with 3.5 or 1.2 cross-links per chain and an M_n up to 14.9 kg mol^{-1} ($Đ$ = 1.5–1.6).[82,84] Subsequently, the branched gels were explored as macroinitiators for chain extension with styrene *via* ATRP. In addition, miktoarm star terpolymers of **poly(MMA-*b*-M13-*b*-BA)** were fabricated *via* an "in–out" methodology (Fig. 16).[83] To achieve this, the synthesis of a **polyMMA** macroinitiator was followed by subsequent chain extension and cross-linking with **M13** to provide degradable star copolymers, which were then again extended using **BA**. Degradation studies revealed that only 19% of the total Br functionality in **poly(MMA-*b*-M13)** was initiated during the ATRP polymerization of **BA**, which was attributed to the high level of core cross-linking. Unfortunately, the occurrence of inter- and intra-star arm–arm couplings was also confirmed.

Stable, hollow polymer nanocapsules with a cross-linked shell were fabricated by ATRP.[85] Firstly, an amphiphilic block copolymer of **PEGMA** and *n*-butyl methacrylate (**BMA**) was obtained and used as macroinitiator in an interfacial miniemulsion copolymerization involving **BMA** and **M13**. As a result, stable nanoparticles were obtained, which after degradation with PBu_3, yielded polymers with an M_n = 34.2 kg mol^{-1} ($Đ$ = 2). It should be noted that relatively high dispersity values were obtained compared to the reference polymer without **M13** incorporation ($Đ$ = 1.5). Furthermore, a sample of **N_3-PEGMA-*b*-PBMA-Cl** was prepared, which possessed a halogen end-group to enable the initiation of ATRP, as well as an azide end-group to enable post-modification (Fig. 17A).[86] Together with monofunctional **PEGMA-*b*-PBMA-Cl**, it was copolymerized with **BMA** and **M13** in a miniemulsion to form nanocapsules with cross-linked shells. Finally, the azide group was reacted with a functionalized dansyl probe in an azide–alkyne cycloaddition, or the polymer was utilized as a macro-ATRP initiator to construct an additional polymer shell (Fig. 17B).

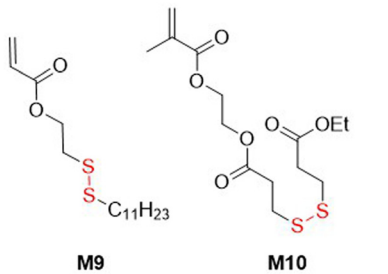

Fig. 14 Monomers with disulfide moiety located in pendant.

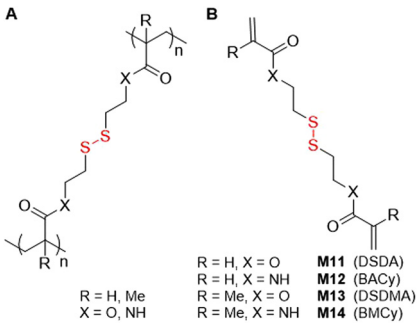

Fig. 15 (A) Polymer containing a disulfide cross-linking monomer; (B) structures of disulfide-containing bifunctional monomers.

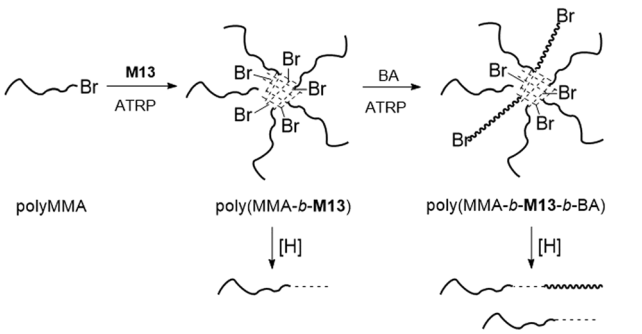

Fig. 16 Synthesis of degradable miktoarm polymers from MMA and M13 and BA *via* ATRP.

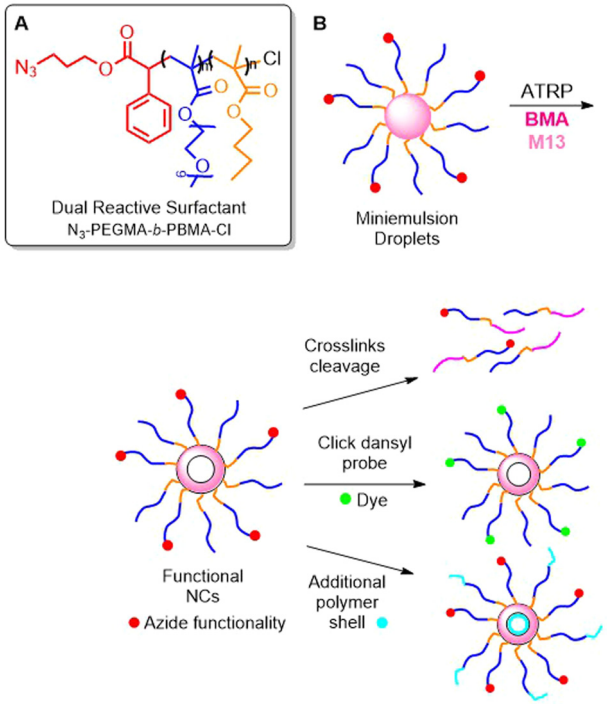

Fig. 17 (A) Structure of dual-functional N3-PEGMA-*b*-PBMA-Cl; (B) scheme of interfacial miniemulsion ATRP of N3-PEGMA-*b*-PBMA-Cl, PEGMA-*b*-PBMA-Cl, BMA and M13 and post-modification.

In addition, monomer **M13** was applied in the synthesis of a disulfide-containing cross-linked star polymer, prepared *via* a core-first methodology (Fig. 18).[7,87] Firstly, ethylene glycol diacrylate (**EGDA**) was homopolymerized under high dilution to prevent macroscopic gelation. When the conversion reached 91%, **BA** was added to produce a **poly(EGDA-*b*-BA)** star polymer with an M_n of *ca.* 375 kg mol^{-1}. This polymer was then subjected to chain extension with cross-linking monomer **M13** to introduce disulfide functionalities into the arm ends.

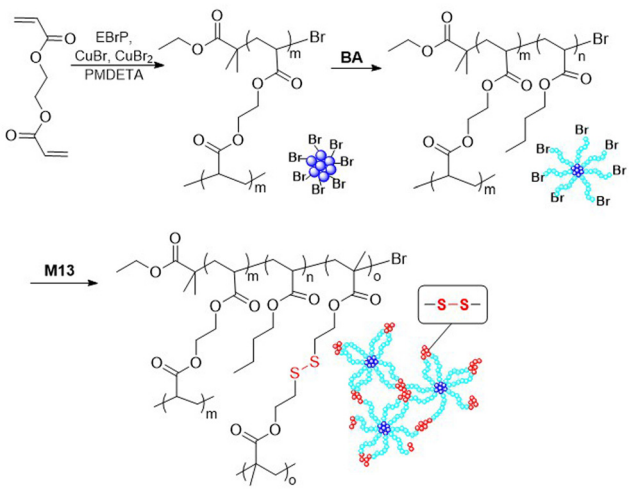

Fig. 18 Synthesis of star polymer poly(EGDA-*b*-BA-*b*-M13).

Treatment with PBu_3 resulted in disulfide bond cleavage to produce individual soluble stars, but under oxidizing conditions the gel could be reformed. In addition, the star polymers in reduced form were deposited on silicon wafer and then oxidized to form an insoluble film which was reported to display self-healing properties.[7]

Next, 2-ethylhexyl methacrylate (**EHMA**) was copolymerized by interfacial miniemulsion ATRP with **M13** to provide a polymer with M_n = 30.5 kg mol^{-1} ($Đ$ = 1.6) containing voids within the macroporous structure ranging from 3–15 μm. Polymerization conditions employing a less hydrophobic catalyst resulted in a non-fully degradable copolymer that contained a less uniform cross-linked network, and lower stiffness and yield strength.[87] Branched copolymers fabricated by the incorporation of **M11** and **M13** were also reported by Armes *et al.*[91–97] Firstly, **HPMA** was copolymerized with **M13** by ATRP.[91] It was confirmed that high levels of **M13** led to macrogelation and an increase in M_n and dispersity. Analysis revealed that the dispersity of the reductively degraded copolymer was analogous to the dispersity of linear **polyHPMA** obtained under the same conditions in the absence of **M13**. Thus, it appeared that high molecular weights were caused mostly by **M13** branching and not by the chain transfer or termination by combination. Based on these results, highly branched, hydrophobic polymers (M_w = 292 kg mol^{-1}) suitable for electrospinning were synthesized.[92]

Then, Armes *et al.* studied the RAFT and ATRP copolymerizations of 2-hydroxypropyl acrylate (**HPA**) with **M13**.[92] For both techniques it was observed that copolymerization involving the cross-linking agent (**M13**) was slower than linear homopolymerization. Interestingly, higher levels of cross-links per chain were incorporated by RAFT before macrogelation occurred. This was explained by the occurrence of intramolecular cyclization of the bifunctional vinyl monomer, instead of intermolecular cross-linking. In further studies on the copolymerization of 2-aminoethyl methacrylate (**AMA**)[94] or **MMA**[95–97] with **M13** it was confirmed that the level of intermolecular cross-linking *versus* intramolecular cyclization was highly dependent upon **M13** concentration and its molar ratio to the CTA. It was reported that intermolecular branches were formed at all monomer concentrations, but that intramolecular cyclization occurs predominantly at a lower feed ratio of **M13** and lower **M13**/CTA molar ratios. Unusually, it was concluded that initial monomer concentration was more important for the microstructure of the polymer product than the polymerization technique.

Tsarevsky *et al.* has studied polymerization of **M13** with functional vinyl monomers in the presence of efficient chain transfer agents.[98,99] Thus, **M13** was copolymerized with diethylene glycol methyl ether methacrylate (**DEGMEMA**),[98] or oligo(ethylene oxide) methyl ether methacrylate (**OEGMEMA**)[98] or ethyl cyanoacrylate (**ETA**) and 2-chloroethyl methacrylate (**ClEMa**)[99] under ATRP conditions with CBr_4 to yield degradable hyperbranched polymers with multiple peripheral alkyl bromide groups. To delay gelation with a large **M13** input in the feed, the ratio of CTA to initiator was raised to up to 40

(for copolymerization with **DEGMEMA** or **OEGMEMA**) or 200 (copolymerization with **ECA** and **CIEMA**). By the addition of *ca.* 5% of crosslinking monomer **poly(DEGMEMA-*co*-M13)** was obtained with M_n = 5.1 kDa ($Đ$ = 3.1). **Poly(DEGMEMA-*co*-M13)** were used as macroinitiators in a copolymerization with **MMA** to yield star copolymers with reductively degradable cores.[98] Tsarevsky *et al.* also obtained hyperbranched disulfide-containing polymers avoiding gelation by the copolymerization of **MMA** and an inimer derived from **M13** but containing an ATRP-initiator moiety.[100]

Paulusse and coworkers obtained **poly(DMAEMA-*co*-M11)** (DMAEMA = *N*,*N*-dimethylaminoethyl methacrylate) in RAFT polymerization.[101] Copolymers with dispersity values <2 were obtained when the process was ended after *ca.* 10 hours, however, when the polymerization was extended to 12 hours, a substantial increase in dispersity ($Đ$ = *ca.* 8.0) and M_n values (from 16.5 to 32.0 kg mol^{-1}) were observed, which supported previous observations regarding branching occurring at higher conversions by RAFT processes.[93] **Poly(DMAEMA-*co*-M11)** was also obtained by ATRP methodology, which after capping with 3-morpholinopropylamine (MPA) was subjected to the formation of polyplexes with plasmid DNA that exhibited good transfection capability.[102] This feature, as well as their cytotoxicity and interaction with nucleic acids, were affected by the degree of branching and the length of the primary-chain molecules. Moreover, by the same technique a larger "knot" structure of cationic polymer **poly(DMAEMA-*co*-M11-*co*-PEGMA)** with 5.6% branching was produced that exhibited a transfection profile for astrocytes that superseded commercially available reagents.[103]

To produce new nanohydrogels as potential platforms for drug delivery, **M12** and **M14** were frequently considered.[74,104–109] Wang and coworkers obtained nanohydrogels in a distillation-precipitation FRP of **MAA** with **M12**.[104] Due to the electrostatic interactions between DOX amine groups and the carboxyl groups incorporated into the nanohydrogels it was possible to load the matrix with up to 42.3 wt% DOX at physiological pH. The DOX-loaded nanohydrogels exhibited pH and redox dual-responsive drug release capabilities, as well as non-toxicity toward normal cell lines, but were reported to have high cytotoxicity to human tumour cells. In addition, **M14** and modified hyaluronic acid (HA) were copolymerized to produce nanogels for DOX encapsulation (Fig. 19).[105] To enable effective penetration of the blood brain barrier, components such as (a) phenylboronic acid (PBA) which displays affinity for sialic acid, and (b) lactoferrin (Lf) which exhibits affinity to receptor-associated proteins which are highly expressed in glioma cancer cells, were incorporated. Studies on drug release, cytotoxicity, cellular uptake, brain permeability and the biodistribution of these nanoassemblies demonstrated their clear superiority to conventional systems.

In 2021, another DOX delivery system was fabricated with **M12** and cyclodextrin (CD) nanosponges used as binding components.[106] Thus, inverse-emulsion FRP polymerization of **AA**, **M12** and acryloyl-6-ethylenediamine-6-deoxy-β-cyclodextrin (**β-CD-NH-ACy**) yielded hyper cross-linked polymer (Fig. 20).

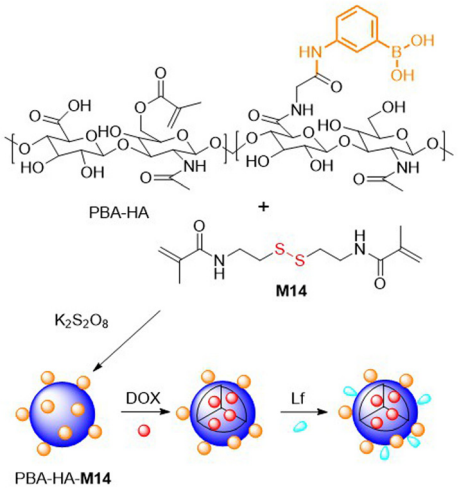

Fig. 19 Schematic synthesis of HA and M14 based nanogel loaded with DOX, designed for effective glioma cell penetration.

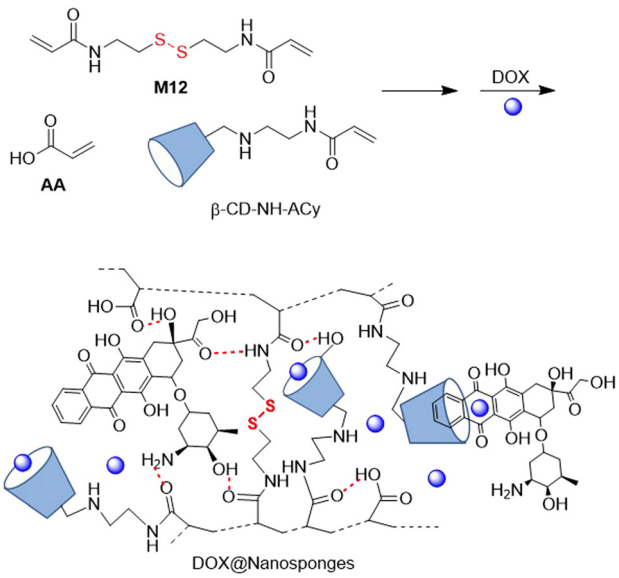

Fig. 20 DOX delivery systems with degradable cyclodextrin (CD) nanosponges.

Further DOX inclusion and complexation with 22.6% drug loading provided spherical-like structures that were responsive to reductive and acidic conditions, effectively releasing DOX at cytosolic GSH levels at a pH of 5.0. These DOX@Nanosponges proved to be cytotoxic against lung cancer cells, in which they were internalized by endocytosis.

Copolymerization of (2-hydroxyethyl) methacrylate (**HEMA**) and **M12** *via* a FRP precipitation-polymerization in water in the presence of cisplatin provided hydrogels imprinted with the anticancer drug.[107] The cisplatin remained complexed with the polymer through hydrogen bonding and was reported to be more effectively released in acidic conditions than at physiological pH. As mentioned in section 2.1.2, **M14** (BMCy) has

also been applied for the synthesis of polymer drug delivery systems involving camptothecin (CPT).[74] Thus, 2,2′-dithiodiethanol methacrylate monomer conjugated with CPT was incorporated to produce block-copolymers **PEG-*b*-poly(MEO$_2$MA-*co*-CPT)-*b*-poly(M14-*co*-BzMA)** *via* RAFT methodology with up to 36.3% of molar drug content (Fig. 12).

Lee and coworkers synthesized copolymers of acrylamide (**AM**) and **M12** as an disulfide moiety-enriched alternative to known copolymers of **AM** and *N*,*N*-methylenebisacrylamide which are exploited for protein resolution during sodium dodecyl sulfate–polyacrylamide gel electrophoresis (SDS-PAGE).[108] The **M12**-based polyacrylamide hydrogel exhibited a higher swelling ratio and pore size than the traditional hydrogel, with comparable capability for protein separation. In addition, RAFT polymerization was utilized to produce branched polymers from poly(ethylene glycol) methacrylate, **M12** and photodegradable monomer 1,3-di(acryloxymethyl)-2-nitrobenzene (**DANB**).[109] After additional hyperbranching in aqueous solution, nanohydrogels were obtained as a result of intermolecular disulfide exchange which exhibited temperature-, photo- and redox-sensitivity.

2.3 Radical ring-opening polymerization (rROP)

Radical ring-opening polymerization (rROP) is a free-radical polymerization technique that involves ring-opening and subsequent propagation involving a cyclic monomer. The harnessing of this technique enables the simple introduction of heteroatom-containing functional groups into a polymer backbone. However, there exists only a few examples within the literature of the utilization of rROP for the synthesis of polymers containing disulfide moieties, being exclusively undertaken using monomer **M15** (MTC) (Fig. 21).[101,110–112] Hawker and coworkers RAFT copolymerized **M15** with **MMA** to provide statistical copolymers possessing reactive disulfide units within the vinyl backbone and *exo*-methylidene groups which could be applied for further functionalization.[110] At all feed ratios, a good agreement between monomer feed ratio and product composition was observed. Moreover, the treatment of the copolymer with sodium methoxide resulted in the decay of the ester groups without affecting the disulfide bonds. Conversely, the disulfide bonds could be selectively degraded in solutions of hydrazine or tributylphosphine.

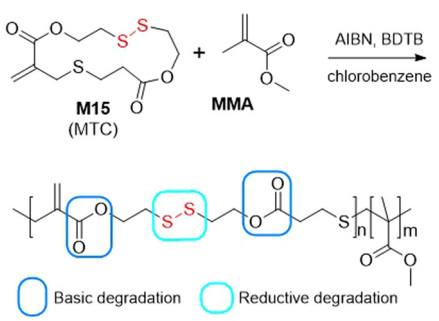

Fig. 21 Synthesis and degradation of poly(MMA-*co*-M15).

Then, Paulusse *et al.* copolymerized **M15** with **HPMA** in the presence of a hydrophilic PGMA$_{56}$ macro-CTA (PGMA = poly(glycerol monomethacrylate) in aqueous solution, with concurrent polymerization-induced self-assembly (PISA) to provide various nanostructures including spheres, worms or vesicles, dependent upon the degree of polymerization (Fig. 22).[111] However, only a small contribution of **M15** in the terpolymer could be introduced without affecting polymer dispersity and nanoparticle morphology. It was concluded that dispersity values of <1.4 could be obtained with a feed ratio of **M15** below 0.5%, and well-defined nanostructures could be formed with an incorporation of **M15** below 1%.

In addition, monomer **M15** was subjected to RAFT copolymerization with DMAEMA and tri(ethyleneglycol) diacrylate (**TEGDA**) (Fig. 23).[101] Polymerization for *ca.* 5 hours provided a controlled linear chain growth without intermolecular cross-linking, until a critical concentration point was achieved during which cross-linking occurred, this process being readily monitored using SEC by a change from unimodal to bimodal signal. Following degradation, a unimodal peak could again

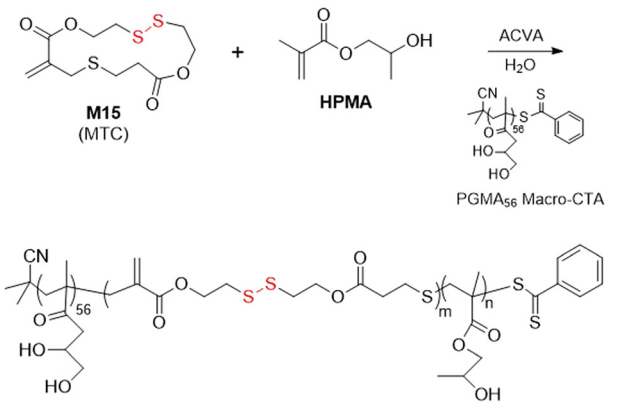

Fig. 22 Synthesis of poly(GMA)-*b*-(M15-*co*-HPMA).

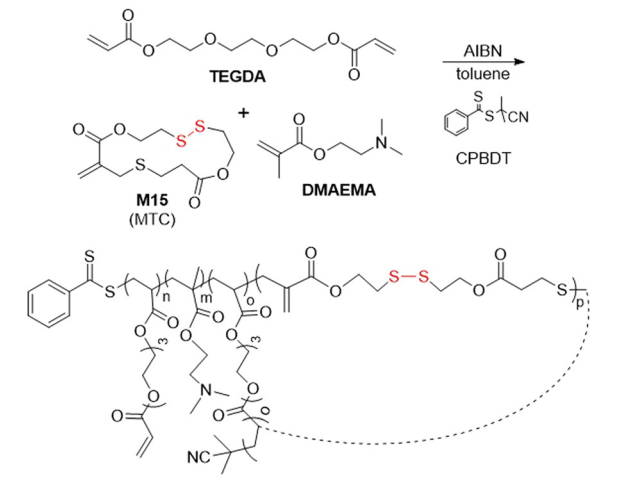

Fig. 23 Synthesis of poly(DMAEMA-*co*-TEGDA-*co*-M15).

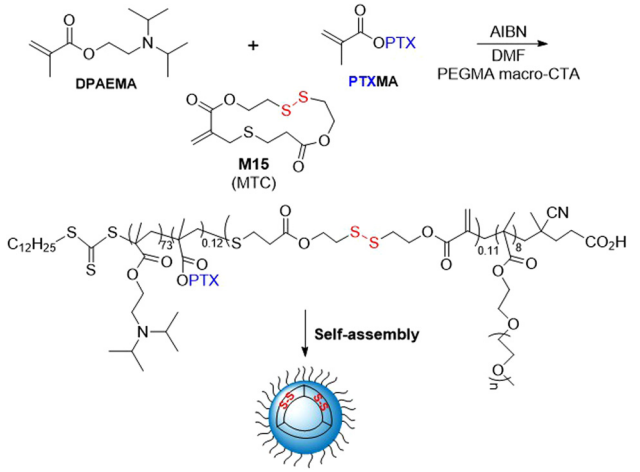

Fig. 24 Synthesis and self-assembly of PEGMA-*b*-(DPAEMA-*co*-PTXMA-*co*-M15).

be observed by SEC analysis, implying a statistical incorporation of **M15** into the polymer backbone. Moreover, this polymer was end-capped with 3-morpholinopropylamine (MPA) and studied as a gene delivery agent for plasmid DNA, displaying improved transfection efficiency and lowered cytotoxicity in comparison to other systems.[102,103]

The RAFT polymerization of anticancer drug paclitaxel conjugated to methacrylate (**PTXMA**), **M15** and 2-(diisopropylamino) ethyl methacrylate (**DPAEMA**) in the presence of a PEGMA macro-CTA provided copolymers with M_n values of 13.6–26.9 kg mol^{-1} ($Đ$ = 1.4–1.5) (Fig. 24).[112] Unfortunately, the final polymer composition of both the **M15** and **PTXMA** was reported to be less than half of the initial feed. By a self-assembly process in water, aggregates having a vesicle shape were obtained. Their anticancer activity was studied *in vitro* and the polymer carrier **PEGMA-*b*-(DPAEMA-*co*-PTXMA-*co*-M15)** was demonstrated to have a higher efficacy than the **PTXMA** monomer.

3. Ring-opening polymerization (ROP)

The application of ring-opening polymerization (ROP) to fabricate polymers containing disulfide moieties is generally represented by processes with an anionic character, and can be performed using *N*-carboxyanhydrides, carbonate, and lactone monomers. The effectiveness of the ROP of lactones and carbonates relies upon the ring-strain of the monomer. For smaller ring heterocycles, the high strain promotes polymerization, while for macrocyclic monomers (≥12 membered) polymerization is frequently more challenging. Moreover, disulfide bonds incorporated into such heterocyclic monomers provide additional limitations in terms of suitable polymerization conditions and catalysts. Nevertheless, there exists multiple reports of effective ROPs of monomers containing disulfide moieties.

3.1 Monomers providing pendant disulfides

Three cysteine derived *N*-carboxyanhydrides (NCAs) with disulfide containing pendants (**M16a–c**) were subjected to ROP to provide polymers with M_n values ranging from 2.5 to 8.3 kg mol^{-1} ($Đ$ = 1.13–1.30) (Fig. 25A).[113] Copolymerization of **M16c** with mPEG$_{45}$-NH$_2$ as a macroinitiator resulted in a block copolymer with an M_n = 11.7 kg mol^{-1} ($Đ$ = 1.1). It was reported that aqueous solutions of this polymer displayed thermal responsivity, but unusually that the reduction in transmittance during the sol–gel transition was not reversible, which was attributed to disulfide bond exchange. Carbonate **M17** and ε-caprolactone (**ε-CL**) were subjected to ROP in the presence of isopropanol as an initiator and Sn(Oct)$_2$ as a catalyst to provide **poly(ε-CL-*co*-M17)** with an M_n = 29.8 kg mol^{-1} ($Đ$ = 1.33) (Fig. 25B).[114] After thiol-exchange with thiolated polyethylene glycol, the resulting biocompatible copolymer was transformed into a doxorubicin-loaded micelle and examined for its cytotoxic activity.

3.2 Monomers providing backbone disulfides

Lee and coworkers performed the ROP of **M18** initiated with alcohol and using diphenylphosphate (DPP) as catalyst (Fig. 26A).[115] In the presence of benzyl, propargyl or isopropyl alcohol, homopolymers were obtained with M_n values up to

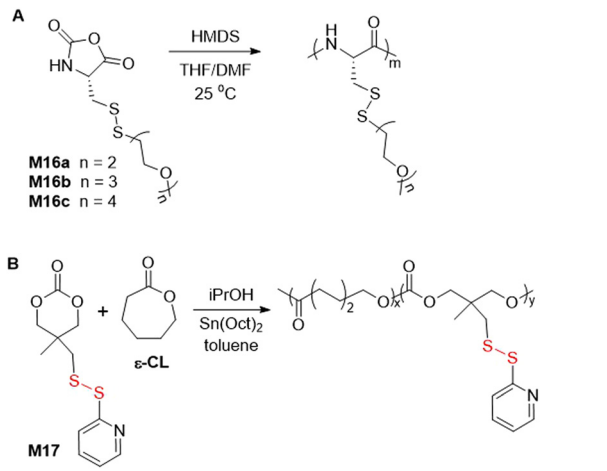

Fig. 25 (A) Synthesis of polyM16; (B) synthesis of poly(ε-CL-*co*-M17).

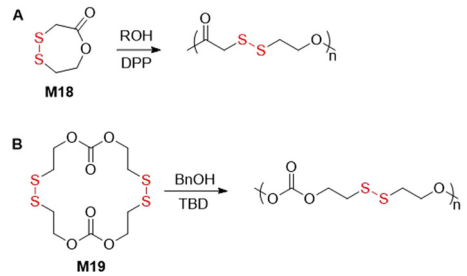

Fig. 26 (A) Synthesis of polyM18; (B) polymerization of macrocyclic carbonate M19.

21.7 kg mol^{-1}, ($Đ$ = *ca.* 1.05) with conversions of >99%. Moreover, polymerizations of **M18** with mPEO-OH (M_n = 2.0 kg mol^{-1}) provided block copolymers. An additional block copolymer was obtained when **M18** was added after complete consumption of **ε-CL**, providing **poly(M18-*b*-ε-CL)** Degradation of this polymer was confirmed under reductive conditions, as well as by UV irradiation. Disulfide-containing macrocyclic carbonate **M19** was also successfully subjected to ROP initiated by benzyl alcohol in the presence of triazabicyclodecene (TBD) to fabricate polymers with M_n values up to 37.2 kg mol^{-1} ($Đ$ = 1.28) (Fig. 26B).[116,117] The activity of the systems was greatly dependent upon the type of organocatalysts applied. It was also reported that chemically catalysed polymerizations displayed the advantage of shorter reaction times at lower temperatures, as well as improved dispersities, in comparison with enzymatic polymerization.[118]

4. Ring-opening metathesis polymerization (ROMP)

Ring-opening metathesis polymerization (ROMP) is a chain-growth strategy for the synthesis of polymers containing carbon–carbon double bonds in the backbone. ROMP is derived from research into olefin metathesis first investigated by Y. Chauvin and later extensively elaborated by R. H. Grubbs. The polymerization process for a broad range of cyclic olefins is characterized by a high selectivity and functional group tolerance, but nevertheless the incorporation of disulfide moieties by ROMP remains problematic. The basis of this issue involves the coordination of the disulfide moiety to the transition metal catalyst.[119] However, multiple reports of the co-polymerization of monomer **M20** with cyclooctanes,[120] or the ROMP of cysteine-based macrocycles **24a/b** appear within the literature.[121–123]

Emrick and coworkers reported the effective copolymerization of **M20** with a series of *cis*-cyclooctane analogues (type **M21**), although the homopolymerization of **M20** was reported ineffective owing to complications involving catalyst coordination (Fig. 27A).[120] Copolymerizations of **M20** and **M21** using Grubbs third generation (G3) catalyst readily provided polymer which was confirmed to contain a random distribution of disulfide moieties. Moreover, a terpolymerization of **M20**, **M21a** and phosphoester monomer **M22** was performed to provide a polymer with orthogonal degradation properties (Fig. 27B).

Schlaad and co-workers reported the ROMP of cysteine-based macrocycles **M24a/b** (Fig. 28).[121–123] Polymerization of **M23a** was attempted with Hoveyda–Grubbs second generation (HG2) catalyst, however only oligomer could be obtained. Monomers **M24a/b** were therefore prepared by ring-closing metathesis (RCM) of the olefinated Boc-l-cysteine dimers **M23a/b**. Following this, the ROMP of **M24a** using G3 catalyst readily provided **polyM24a** with an M_n = 10.5 kg mol^{-1} ($Đ$ = 2.2). Since these monomers exhibited low ring-strain, their polymerization was conducted at high concentration in order to obtain favorable entropy. Moreover, it was postulated that

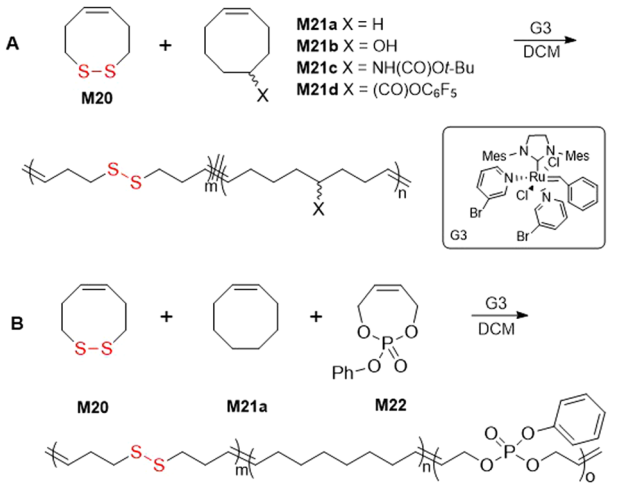

Fig. 27 (A) Copolymerization of M20 with *cis*-cyclooctanes M21a–d; (B) terpolymerization of M20 with M21a and phosphoester M22.

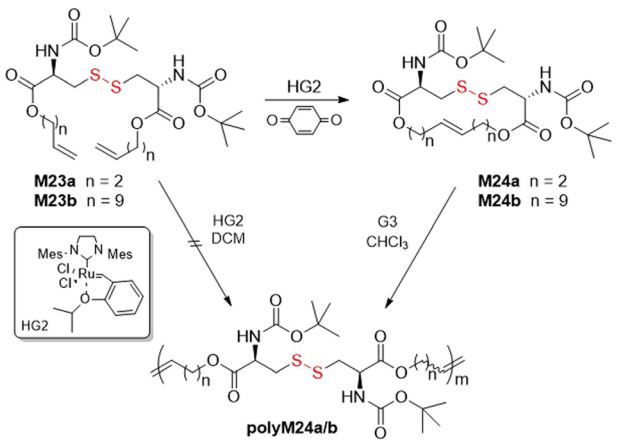

Fig. 28 ROMP of macrocycles M24a/b.

the disulfide bonds had little effect on the polymerization owing to the significant distance between the catalyst site and disulfide bond location.

5. Miscellaneous

5.1 Radical ring-opening polymerization of the disulfide bond – thermal- and photo-initiated

The first reports regarding the radical ring-opening polymerization of disulfide-containing monomers actually referred to naturally occurring lipoic acid (**M1**) and were comprised of reactions initiated by heat or irradiation (Fig. 29). In 1955, it was serendipitously discovered by Niu and Reed that **M1** could undergo polymerization during the oxidative conditions that were required for its synthesis.[124] Later, **M1** was purposely polymerized at 65 °C to provide a colourless material which could be decomposed using NaOH to recover monomer.[125] Calvin and coworkers simultaneously explored the photo-

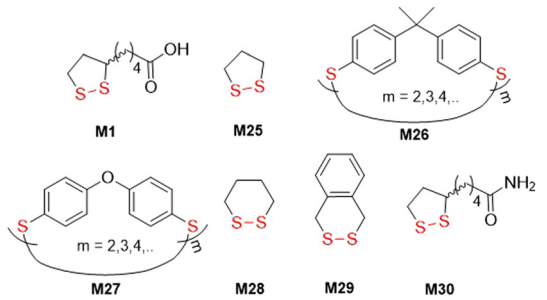

Fig. 29 Cyclic disulfide monomers used for thermal- and photo-induced radical ring-opening polymerizations.

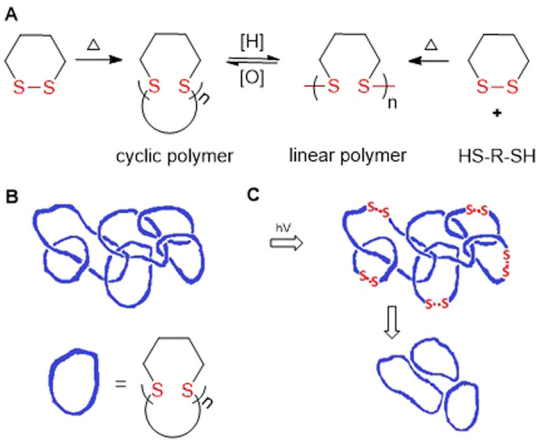

Fig. 30 (A) Polymerization of 1,2-dithianes in initiator-free conditions *versus* thiol-mediated reactions leading to cyclic or linear polymers, respectively; (B) polycatenane structure of poly(disulfide)s; (C) photo-induced degradation leading to non-entangled cyclic polymer formation.

polymerization of 1,2-dithiolane monomers **M1** and **M25**, demonstrating that irradiating these monomers results in diradical formation and subsequent polymerization in neutral solution.[126] Conversely, in acidified solution the dithiolane ring was destroyed to yield thiol and sulfenic acid, with no polymerization.

Hay and coworkers later reported the thermally-induced radical copolymerization of macrocyclic aromatic disulfides **M26** and **M27** (both consisting of mixed quantities of oligomer).[127–131] It was reported that the melt homopolymerization of oligomeric **M26** was possible above its melting point, and was rapid at 200 °C, providing **polyM26** with M_n = 88.0 kg mol^{-1} ($Đ$ = 2.15).[128] Moreover, solution polymerization also provided **polyM26** with M_n = 64.0 kg mol^{-1} ($Đ$ = 1.92). For both processes, the M_n and dispersity remained relatively stable for short reaction times, but at high temperatures (>250 °C) or after prolonged reaction time the occurrence of substantial cross-linking was confirmed. Endo and coworkers reported the thermally-induced rROP of **M28**/**M29**,[132–135] **M1**,[136] and the copolymerization of **M28** and **M1**.[137,138] It was demonstrated that these monomers can polymerize in bulk without an initiator when held above their melting point, but that cyclic polymers were formed by a back-biting mechanism (Fig. 30A).[133,135–137] Furthermore, it was established that these conditions provided entangled polycatenane macrostructures (Fig. 30B). Photoinduced degradation in dilute solution led to a loss in molecular weight, but also the preservation of cyclic character, attributed to the disconnection of the polycatenane structure (Fig. 30C).

Bulk polymerization of **M29** at 90 °C led to cyclic polymer with an M_n = 11.8 kg mol^{-1} ($Đ$ = 1.95), characterized by higher thermal stability and lower crystallinity than **polyM28**.[135] Likewise, the bulk polymerization of **M1** at 90 °C produced a cyclic polymer with M_n = 13.7 kg mol^{-1} ($Đ$ = 1.5) in 67% yield.[136] Interestingly, bulk polymerization in the presence of 6,8-dimercapto-octanoic acid (DHLA) at 120 °C provided a linear polymer with an M_n = 9.1 ($Đ$ = 2.7), but with significantly lower monomer conversion. Bulk copolymerization of **M28** and **M1** at 80 °C with varying feed ratios led to a series of random sequence copolymers with M_n = 20.1–55.0 kg mol^{-1} ($Đ$ = 1.45–2.35).[137] Due to the difference in ring-strain energies, monomer conversion increased with an increase in **M1** feed, which was also more frequently incorporated into the copolymer than **M28**. Endo also performed thermally-induced copolymerizations of lipoamide **M30** and styrene in solution.[139] An increase in the feed ratio of **M30** resulted in a decrease in conversion, and no polymer was obtained at 50 mol% **M30** feed. Differences in the reactivity between the polymeric thiyl and polystyryl radicals during propagation, as well as chain transfer to the amide group, were suspected of causing retardation of the copolymerization. Conversely, if a solution of **M30** and styrene was irradiated with UV light at 40 °C, copolymers with enriched **M30** relative to the feed were produced.[139] Interestingly, irradiation of a solution of styrene produced only traces of polymer, unlike the copolymerization which was presumably initiated by a homolytic fission of **M30** to produce initiating diradical species.

Recently, it was demonstrated that photo-induced polymerization without solvent could also provide interlocked products.[140] Therefore, **M1** was melted at 120 °C to provide a transparent liquid, which during cooling provided a transparent yellow polymer gel, followed by crystallization of the unreacted **M1**. Then, by irradiation with UV/visible light, polymerization of the remaining monomers occurred to give a colourless film consisting of interlocked cyclic poly(disulfide)s which could be converted by thermal depolymerization to starting monomer. Macromonomers **M31** and **M32**, consisting of lipoates containing poly(dimethylsiloxane) fragments, were irradiated with UV light to provide bottlebrush polymers in a grafting-through polymerization strategy (Fig. 31A).[141] After subjection to thermal depolymerization, *ca.* 30–40% of the original monomer (**M31**) could be recovered. Irradiation-induced copolymerization of **M33** with cross-linker poly(ethylene glycol)-diacrylate in the presence of a photoinitiator provided material that was used as resin for 3D printing, capable of both thermal and photo-induced reprocessing (Fig. 31B).[142]

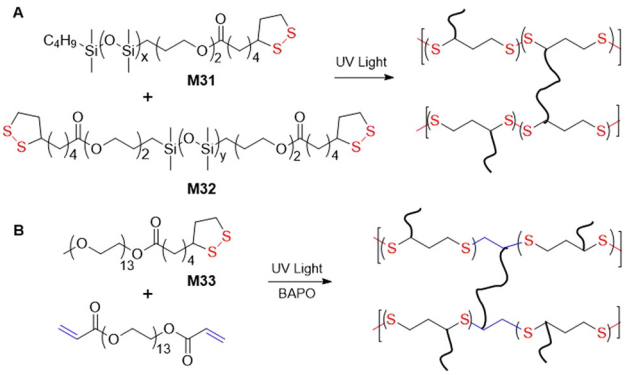

Fig. 31 Light-mediated synthesis of dynamic bottlebrush elastomers from lipoic acid-based monomers M31–33.

Orthogonal monomers containing vinyl or acrylate groups linked with lipoic or asparagusic acid moieties can be polymerized to provide linear polymers with intact pendant disulfide units which can then undergo photoinduced polymerization to lead to gelation. For example, **M34** was copolymerized with **BMA** to form a linear polymer with M_n values of 17.0–21.0 kg mol^{-1} ($Đ$ = 1.36–1.63) (Fig. 32).[143] The disulfide bonds within the **poly(BMA-*co*-M34)** were then cleaved and recombined using UV irradiation to provide a cross-linked network. In addition, monomer **M35** was subjected to cationic polymerization of the alkene bonds to provide linear polymers containing pendant disulfide units in the side chain (M_n = 1.3 kg mol^{-1}, $Đ$ = 2.5).[144] Conversely, when **M35** was subjected to radical photopolymerization, branched macromolecules were formed due to the ability of the reactive functionalities to undergo both radical polymerization and thiol–ene coupling.

5.2 Radical ring-opening polymerization of the disulfide bond – radically initiated

The polymerization of 1,2-dithiolanes by free-radical initiation has only been modestly reported since it displays several limitations. The radical-initiated homopolymerization of disulfide monomers is reported troublesome, while copolymerization with vinyl comonomers is more efficient, and indeed some reports have been published.[145] However, disulfide linkages can only be incorporated into a polymer backbone when two disulfide-containing monomers are added in succession during propagation, and conversely, only monosulfides are installed when a disulfide monomer is preceded or followed by a vinyl monomer, making this methodology less attractive.

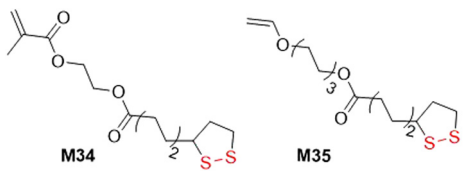

Fig. 32 Orthogonal monomers with methacrylate/vinyl and 1,2-dithiolane functionality.

In 1953, **M37** was copolymerized with vinyl acetate (**VAc**)[146] or styrene[147] to produce polymers with disulfide linkages in the polymer backbone (Fig. 33). Then, Endo and coworkers subjected **M30** to copolymerizations with styrene, acrylonitrile, methyl acrylate, **VAc**, and **MMA** in the presence of AIBN, with disulfide monomer feed ratios of 15 mol%.[145] Copolymerization was reported to occur in all cases, except for the polymerization with **MMA** which provided only **polyMMA** homopolymer, attributed to steric hindrance. For the copolymerization with **VAc**, the final content of **M30** was enriched compared to the feed, with the opposite true for the other monomers.

Tang and Tsarevsky selected specific monomers able to form radicals that were reactive toward 1,2-dithiolane monomers.[148] Thereby, copolymerizations of equimolar mixtures of ethyl acrylate (**EA**) and **M1** or **M36** to fabricate **poly(EA-*co*-M1)** and **poly(EA-*co*-M36)**, respectively, containing significant quantities of disulfide bonds were performed (Fig. 34).[149] Moreover, orthogonal monomer **M38** also yielded polymer with disulfide bonds within the polymer backbone. After treatment with DTT, partial degradation was observed alongside an increase in the molecular weight, attributed to thiol–ene reactions between thiol radicals and pendant vinyl groups.

Recently, it was demonstrated that **M36** can undergo radical polymerization in bulk or in solution with limited conversion which was lowered further with a rise in temperature or dilution.[149] Consequently, it was established that there exists

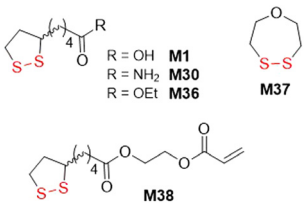

Fig. 33 Disulfide monomers in radical ring-opening polymerization induced with a radical initiator.

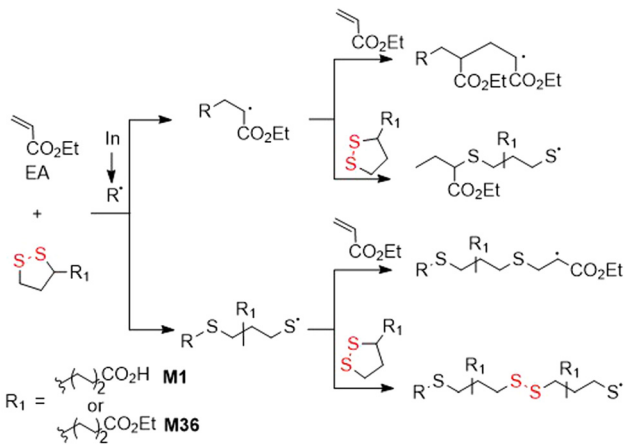

Fig. 34 Copolymerization of EA with M1 or M36.

for **M36** a monomer–polymer equilibrium with a ceiling temperature of 139 °C.

5.3 Ring-opening polymerization of the disulfide bond – thiolate initiated

The thiolate-initiated anionic ROP of disulfide-containing cyclic monomers is based upon the capability of thiols to act as a nucleophile, breaking the disulfide bond to initiate propagation (Fig. 35). This process can be thermodynamically controlled since the thiolate-disulfide exchange is reversible. All reports within the literature relate to 5- and 6- membered cyclic monomers. Endo and co-workers reported that small amounts of benzyl mercaptan (*ca.* 0.8 mol%) added to the bulk polymerization of **M28** at 80 °C resulting in decreased yields from 84 to 3% when compared to bulk polymerization without thiol initiator.[133,134] More versatile studies regarding the incorporation of thiolate initiators were performed using lipoic and asparagusic acid derivatives. In surface-initiated polymerizations, Matile *et al.* obtained poly(disulfide)s from 1,2-dithiolane monomers **M39–M44** (Fig. 35).[150,151] In these studies, *N*-acetyl-l-cysteine methyl ester (Ac-Cys-OMe) and a variety of fluorescent thiols were used as initiators, and iodoacetamides as terminators. Thiol-initiated homopolymerizations were straightforward in terms of control and optimization. Polymerizations of **M39** with Ac-Cys-OMe performed in aqueous solution led to polymer with an M_n = 34.3 kg mol^{-1} ($Đ$ = 1.83) in less than 5 minutes. In addition, the polymerization of **M42** and **M43** was reported troublesome as these monomers are highly reactive and readily polymerize without an initiator. Cellular uptake studies demonstrated that these cell-penetrating polymers can reach the cytosol of HeLa cells and depolymerize, releasing an active payload.

Waymouth *et al.* studied kinetic and thermodynamic differences in the thiol-initiated ring-opening polymerization of 1,2-dithiolanes in regard to the role played by substituents (Fig. 36).[152] The methyl ester of methyl substituted asparagusic acid (**M45**) and methyl lipoate (**M46**) were compared by benzyl mercaptan-initiated polymerization. It was demonstrated that the polymerization is completely reversible, and that conversion is dictated by a thermodynamic polymerization–depolymerization equilibria. Due to high equilibrium monomer concentration $[M]_{eq}$ values, a high initial dithiolane concentration ($[M]_0 > [M]_{eq}$) was required for ring-opening polymerization to occur. Additionally, it was established that equilibrium constants (K_{eq}) in the ring-opening polymerization of **M46** was 3.2 higher than for the same process of **M45**. Based on the observed rate constant it was determined that the propagation rate of **M45** is *ca.* 4.5 faster, and that the depropagation rate is *ca.* 14 faster, than **M46**.

In 2019, Moore and coworkers reported a topology-controlled polymerization of **M46**, based upon the structure of the thiol initiator (Fig. 37).[153] It was reported that predominantly cyclic products were obtained in polymerizations performed using thiophenol initiators, while prominently linear products were obtained for alkyl thiolate-initiated polymerizations. Using a thiophenol initiator with a monomer to initiator ratios

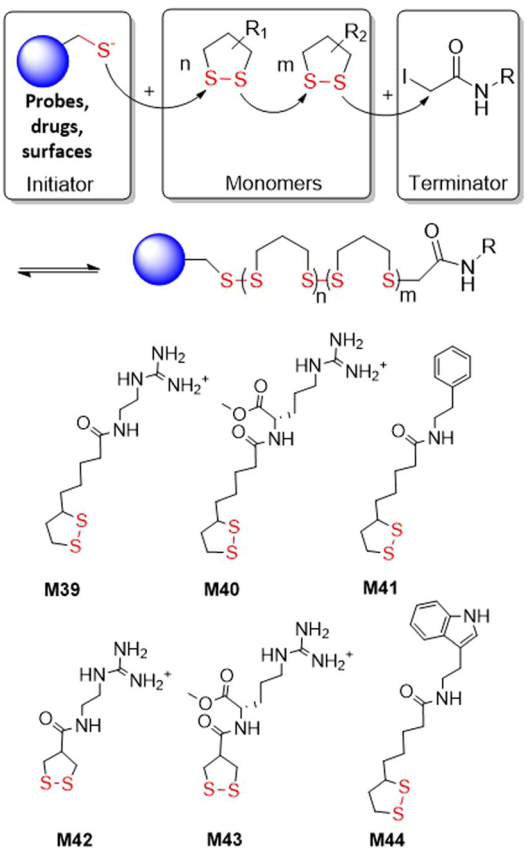

Fig. 35 Polymerization from 1,2-dithiolane monomers M39–M44.

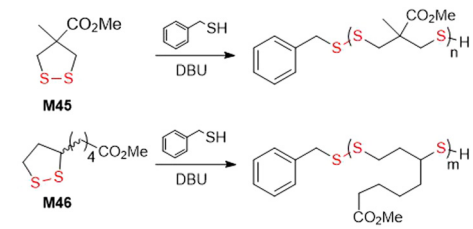

Fig. 36 Benzyl mercaptan initiated polymerization of 1,2-dithiolanes M45 an M46.

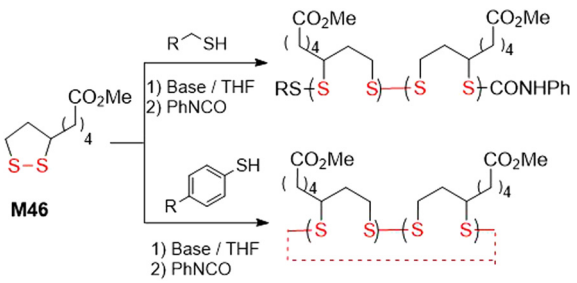

Fig. 37 Copolymerization of M46 initiated with aryl and alkyl thiols.

of 100 : 1, respectively, polymer with an M_n = 22–65 kg mol^{-1} ($Đ$ = *ca.* 1.4) could be obtained, while applying a 5000 : 1 ratio provided polymer with an M_n value as high as 630 kg mol^{-1} ($Đ$ = 1.27). In polymerizations applying alkyl thiols, products characterized by an M_n of 15–18 kg mol^{-1} ($Đ$ = *ca.* 1.4) were produced. Polymerizations performed using **(*R*)-M46** demonstrated a non-regioselectivity of the ring-opening process. Moreover, the kinetics of the polymerization of **M46** turned out to be highly dependent upon the choice of base.

Lu and coworkers performed a rapid and controlled ROP of water-soluble 1,2-dithiolanes **M47–M49** initiated by green fluorescence protein (GFP) at temperatures below 0 °C (Fig. 38).[154] Low polymerization temperatures were reported necessary to address problems relating to high $[M]_{eq}$ value, side reactions, and a loss of protein function. For cryo-polymerization (from 0 to −30 °C), high initiation efficiency of up to 95% was obtained at pH ≥6.5. Polymers with increasing M_n values were obtained with a decrease in polymerization temperature to −30 °C and a rise in pH value to 7.5–8.5. It was reported that a protein-polymer conjugate of **M49** with an M_n = 55 kg mol^{-1} could be obtained after 90 min at −30 °C.

In addition to ROMP (Fig. 28), Schlaad and coworkers also performed the thiolate-initiated polymerization of monomer **M24a** *via* the metathesis of its disulfide group (Fig. 39A).[122] In a polymerization initiated with methyl thioglycolate and triethylamine, **poly(M24a)′** with an M_w = 53–60 kg mol^{-1} ($Đ$ = 1.8) was obtained. Reaction equilibrium was achieved in less than 5 minutes, with a monomer conversion of *ca.* 75%. The chemical structures of **polyM24a** and **polyM24a′** were identical (with the exception of the end-group), with a similar distribution of *cis*/*trans* isomers. Kinetic investigations confirmed that both ring-opening polymerizations were entropy driven.[123] However, while the disulfide metathesis pathway enabled the synthesis of polymers with M_w values up to 180 kg mol^{-1}, olefin metathesis yielded polymers with a maximum M_w value of only ∼70 kg mol^{-1}. In addition, an analogous polymer **polyM50**, with an amide group in the place of the ester moiety, was obtained from monomer **M50** with an M_w = 44 kg mol^{-1} ($Đ$ = 3.5) and monomer conversion of 87% after 1 h (Fig. 39B).

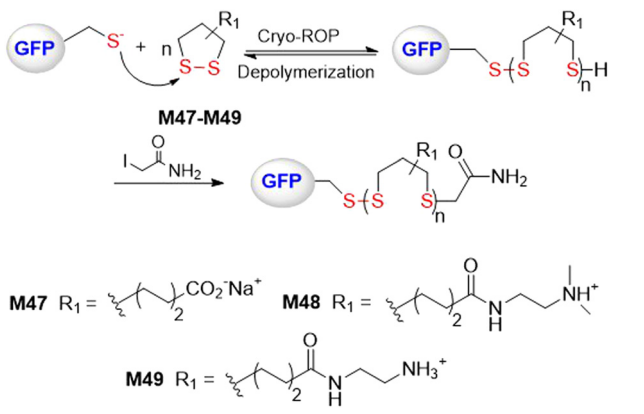

Fig. 38 ROP of water-soluble 1,2-dithiolanes M47–M49 initiated by green fluorescence protein (GFP) at low temperatures.

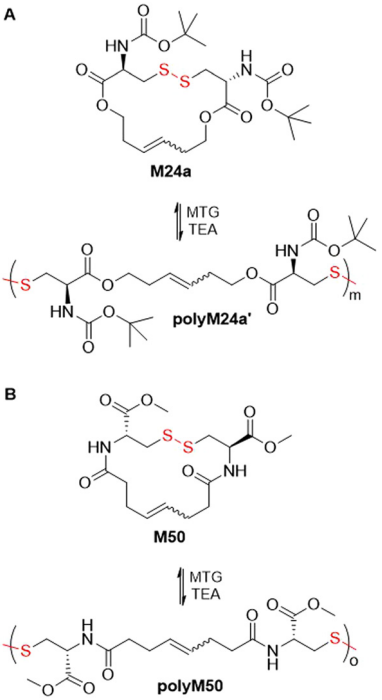

Fig. 39 (A) Polymerization of L-cysteine derived monomer M24a *via* disulfide bond metathesis; (B) polymerization of monomer M50 *via* disulfide bond metathesis.

Polydisulfide-based covalent adaptable liquid crystal networks (CA-LCNs) were obtained from lipoic acid derived monomers **M51**/**M52** *via* thiolate-initiated ROP (Fig. 40).[155] Thus, equimolar mixtures of monomers were copolymerized in the presence of 1,6-hexanedithiol and TBD to fabricate self-healing polydisulfide films that displayed reversible shape programmability. In addition, the polymer underwent effective depolymer-

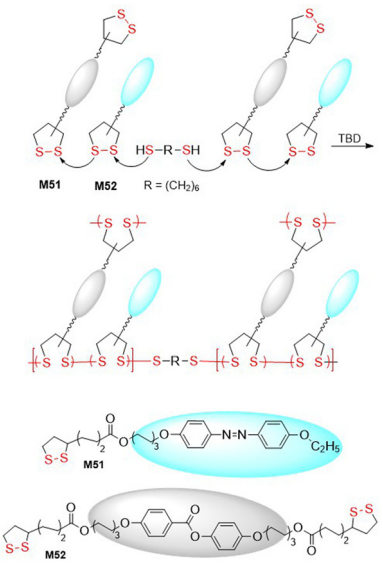

Fig. 40 Synthesis of CA-LCNs from monomers M51 and M52.

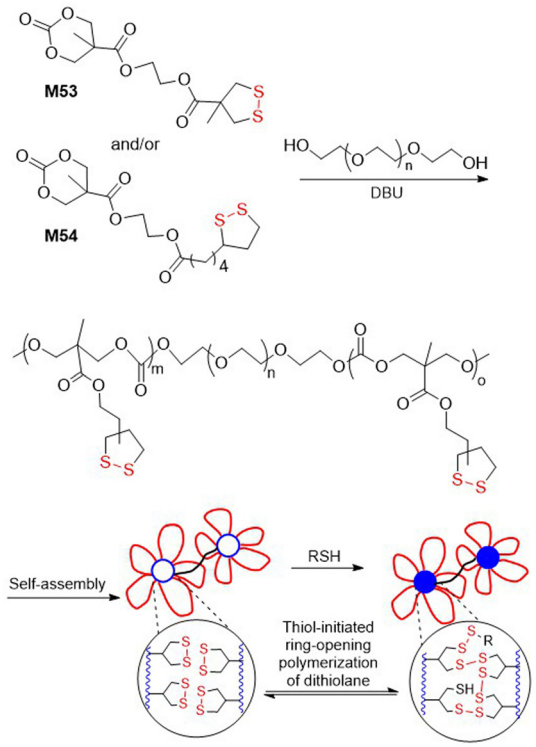

Fig. 41 Polymerization of M53 and M54 followed by self-assembly and thiolate-initiated gelation.

ization into monomer, followed by repolymerization, thereby demonstrating full chemically recyclable behaviour. A thiolate-initiated reversible ROP was also applied for the hydrogelation of polymers containing asparagusic or lipoic acid-derived pendants obtained from monomers **M53** and **M54** (Fig. 41).[156] These cyclic carbonates were subjected to ROP using PEG (14 kg mol^{-1}) as a divalent macroinitiator to fabricate amphiphilic ABA-type triblock polymers with an M_n = 16.9–18.2 kg mol^{-1} ($Đ$ = 1.13–1.18). These polymers then underwent self-assembly in aqueous solution to form flower-like micelles, with the asparagusic acid-derived hydrogels displaying greater dynamic properties, adaptability, and self-healing than those derived from lipoic acid.

6. Common methods for the preparation of disulfide-containing monomers

Disulfide bonds are typically formed by the oxidation of sulfhydryl (-SH) groups (Fig. 42A) or by disulfide-thiol exchange (Fig. 42B). Alternative more specific methods instead apply substrates that contain an equivalent of an "–S$^+$" moiety, for example sulfenyl chlorides or Bunte salts (Fig. 42C).[157,158] Typically, the first two methodologies were applied for the synthesis of the monomers within this article. Moreover, the disulfide bond formation was typically performed as the final

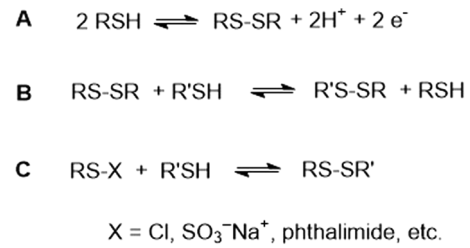

Fig. 42 Common methods for the synthesis of disulfide-containing molecules.

step in the synthetic pathway, or more rarely, in an earlier step which was followed by simple transformations.

An overview of several common approaches for the synthesis of disulfide-containing monomers is herewith provided (Fig. 43). An oxidation approach was applied for the synthesis of thioctic acid **M1** obtained from compound **55** in the presence of iron chloride,[159] or iodine and potassium iodide[159,160] (Fig. 43A). Monomer **M20** was obtained by the air-oxidation of compound **56** mediated by CsF-impregnated Celite (Fig. 43B).[161] Several disulfide-containing monomers were derived from compounds **58** or **60**, which are obtained by oxidation of **57** and **59**, respectively (Fig. 43C).[162,163] Acylation of the resulting diol (**58**) or diamine (**60**) with acryloyl **61**[164,165]

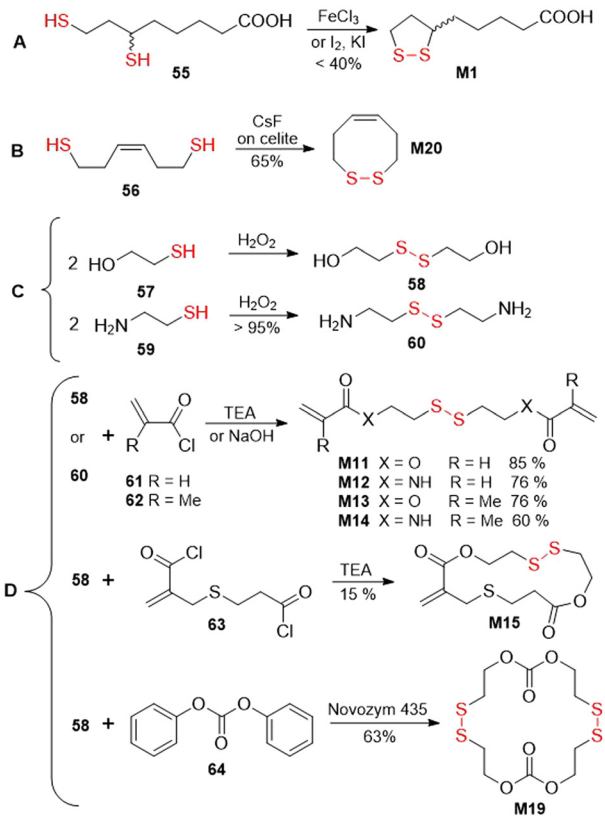

Fig. 43 Oxidation approach used in synthesis of disulfide-containing monomers.

and methacryloyl **62**[105,166] chlorides produces bifunctional vinyl monomers **M11–M14**, which have been applied for cross-linking during FRP (Fig. 43D). Furthermore, by the reaction of **58** with bis-acid chloride **63**, macrocyclic monomer **M15** was obtained in 15% yield.[110] The application of the same diol (**58**) in a reaction with diphenylcarbonate **64** in the presence of lipase enzyme provided monomer **M19** in 63% yield.[118]

Alternatively, a disulfide-thiol exchange approach was applied for the synthesis of pyridyl disulfide functionalized monomers **M3–M6** (Fig. 44A). In this way, 2,2′-dipyridyldisulfide **65** was subjected to substitution with 2-hydroxyethanethiol **57** or 2-mercaptoethylamine **59** to provide compounds **66**[167] or **67**,[168] respectively, with concurrent release of pyridine-2-thione. These intermediates were then reacted with acryloyl (**61**)[44,49] or methacryloyl (**62**)[16,56] chlorides to efficiently provide monomers **M3–M6**. Similarly, for the synthesis of monomer **M9**, compound **68** was subjected to substitution with compound **69** and the resulting intermediate (**70**) was reacted with 2-hydroxyethanethiol (**57**) to provide disulfide **71**, which was finally acylated with acryloyl chloride (**61**) to provide monomer **M9** (Fig. 44B).[76]

The final alternative approach involves the reaction of thiols with various reagents delivering equivalents of "–S$^+$", leading to asymmetrical disulfides. For example, the thiol group of L-cysteine (**73**) was ligated with sulfenyl chlorides **72a–c** to provide cysteine derivatives **74a–c** in good yields, which were then converted into the corresponding *N*-carboxyanhydrides **M16a–c** by their reaction with triphosgene (Fig. 45).[113]

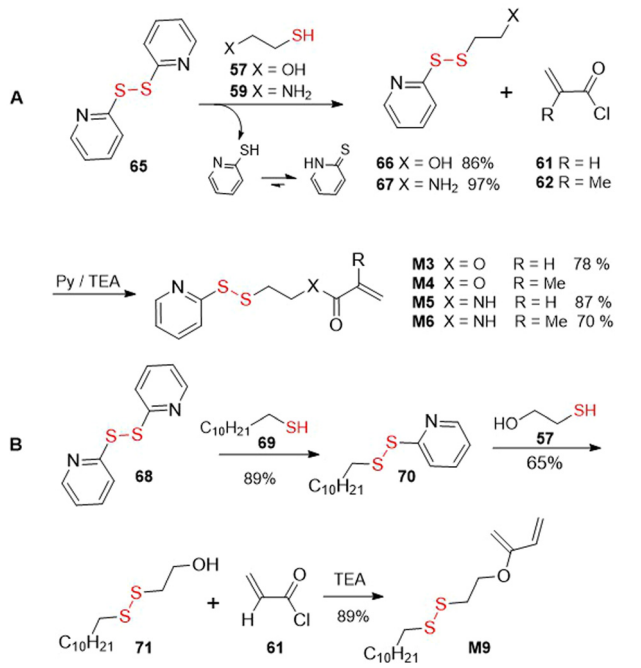

Fig. 44 Disulfide-thiol exchange approach in synthesis of disulfide-containing monomers.

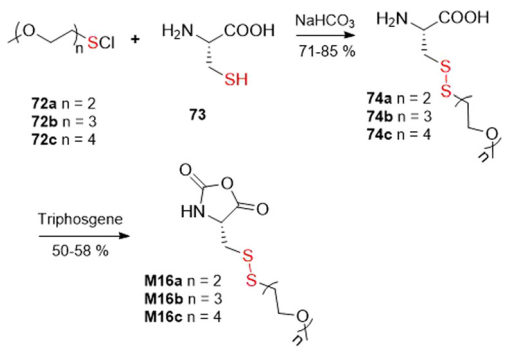

Fig. 45 Approach utilizing the equivalent of an "–S+" moiety for the synthesis of disulfide-containing monomers.

7. Conclusion and outlook

Within this review article we have attempted to provide a comprehensive overview of the diversity of disulfide-containing polymers that can be obtained by chain-growth polymerization by the application of disulfide-containing monomers. As the installation of disulfide moieties into polymers furnishes them with highly useful properties that greatly extend their spectrum of applications, it is of great importance to develop new effective ways to introduce disulfide bonds into polymers. The transfer of disulfide moieties from monomer to (co)polymer is possible *via* a variety of chain-growth polymerization methodologies. These technologies include: (a) radical polymerization by which disulfide bonds can be introduced into pendant groups by FRP, or into the polymer backbone by rROP, (b) ionic ROP performed using cyclic *N*-carboanhydrides, carbonates and lactones, or (c) the ROMP of cyclic disulfide-containing olefins. Moreover, the polymerization of various compounds by the direct ring-opening of the disulfide-bond by an assortment of triggers including thermal, light, anionic and radicals has provided dynamic materials with high levels of chemical recyclability.

Many of the disulfide-containing copolymers discussed herein have been obtained from monomers equipped with active drug molecules, or have been chemically modified with active compounds, and/or conjugated or complexed with proteins and nucleic acid. These polymers have been applied for the fabrication of various nanoarchitectures that have been demonstrated to have increased selectivity, biocompatibility, or transfection ability. The sensitivity of disulfide bonds to reducing conditions has been extensively exploited in research relating to the targeted delivery of active molecules, designed to take advantage of variations in glutathione levels between normal and abnormal cells. In addition, by the application of 1,2-dithiolane monomers, new smart materials with self-healing capabilities, stimuli-responsiveness, adaptiveness, and recyclability have been reported. The effective incorporation of disulfide bonds into a polymer backbone also offers the possibility to obtain new (bio)degradable polymers.

However, the field of disulfide-containing polymers still remains in the initial stages of exploration, and at present, exists predominantly on the bench scale, often facing complications involving tedious monomer synthesis, problematic polymerization, and low monomer incorporation. Nevertheless, the exploration of disulfide-containing polymers remains an extremely active field, and we expect that the future will be a theatre of important innovations regarding the synthesis of new disulfide-containing monomer building blocks that are capable of providing next-generation smart materials that incorporate improved stimuli-responsiveness, degradability, and recyclability.

Conflicts of interest

There are no conflicts to declare.

Acknowledgements

This research was conducted as a part of the International Research Agendas PLUS programme of the Foundation for Polish Science, co-financed by the European Union under the European Regional Development Fund (MAB PLUS/2019/11).

References

1 A. G. Gaydon, *Dissociation energies and spectra of biatomic molecules*, Chapman and Hall, London, 2nd edn, 1953.
2 D. Fass and C. Thorpe, *Chem. Rev.*, 2018, **118**, 1169–1198.
3 S. C. Mitchell and R. H. Waring, *Phytochemistry*, 2014, **97**, 5–10.
4 L. Teuber, *Sulfur Rep.*, 1990, **9**, 257–333.
5 C.-S. Jiang, W. E. G. Müller, H. C. Schröder and Y.-W. Guo, *Chem. Rev.*, 2011, **112**, 2179–2207.
6 K. Kishore and K. Ganesh, *Adv. Polym. Sci.*, 1995, **121**, 81–121.
7 J. A. Yoon, J. Kamada, K. Koynov, J. Mohin, R. Nicolaÿ, Y. Zhang, A. C. Balazs, T. Kowalewski and K. Matyjaszewski, *Macromolecules*, 2012, **45**, 142–149.
8 M. Pepels, I. Filot, B. Klumperman and H. Goossens, *Polym. Chem.*, 2013, **4**, 4955–4965.
9 I. Azcune and I. Odriozola, *Eur. Polym. J.*, 2016, **84**, 147–160.
10 J. F. Quinn, M. R. Whittaker and T. P. Davis, *Polym. Chem.*, 2017, **8**, 97.
11 B. van Lierop, S. C. Ong, A. Belgi, C. Delaine, S. Andrikopoulos, N. L. Haworth, J. G. Menting, M. C. Lawrence, A. J. Robinson and B. E. Forbes, *Sci. Rep.*, 2017, **7**, 17239.
12 B. Sui, C. Cheng and P. Xu, *Adv. Ther.*, 2019, **2**, 1900062.
13 L. Wang, J. Kristensen and D. E. Ruffner, *Bioconjugate Chem.*, 1998, **9**, 749–757.
14 V. Bulmus, M. Woodward, L. Lin, N. Murthy, P. Stayton and A. Hoffman, *J. Controlled Release*, 2003, **93**, 105–120.
15 M. E. H. El-Sayed, A. S. Hoffman and P. S. Stayton, *J. Controlled Release*, 2005, **101**, 47–58.
16 S. Ghosh, S. Basu and S. Thayumanavan, *Macromolecules*, 2006, **39**, 5595–5597.
17 L. Wong, C. Boyer, Z. Jia, H. M. Zareie, T. P. Davis and V. Bulmus, *Biomacromolecules*, 2008, **9**, 1934–1944.
18 Z. Jia, L. Wong, T. P. Davis and V. Bulmus, *Biomacromolecules*, 2008, **9**, 3106–3113.
19 J. H. Ryu, S. Jiwpanich, R. Chacko, S. Bickerton and S. Thayumanavan, *J. Am. Chem. Soc.*, 2010, **132**, 8246–8247.
20 J. H. Ryu, R. T. Chacko, S. Jiwpanich, S. Bickerton, R. P. Babu and S. Thayumanavan, *J. Am. Chem. Soc.*, 2010, **132**, 17227–17235.
21 S. Jiwpanich, J. H. Ryu, S. Bickerton and S. Thayumanavan, *J. Am. Chem. Soc.*, 2010, **132**, 10683–10685.
22 D. C. González-Toro, J. H. Ryu, R. T. Chacko, J. Zhuang and S. Thayumanavan, *J. Am. Chem. Soc.*, 2012, **134**, 6964–6967.
23 L. Li, J.-H. Ryu and S. Thayumanavan, *Langmuir*, 2012, **29**, 50–55.
24 N. M. Matsumoto, D. C. González-Toro, R. T. Chacko, H. D. Maynard and S. Thayumanavan, *Polym. Chem.*, 2013, **4**, 2464–2469.
25 X. Liu, D. Hu, Z. Jiang, J. Zhuang, Y. Xu, X. Guo and S. Thayumanavan, *Macromolecules*, 2016, **49**, 6186–6192.
26 J.-H. Ryu, S. Bickerton, J. Zhuang and S. Thayumanavan, *Biomacromolecules*, 2012, **13**, 1515–1522.
27 L. Li, K. Raghupathi, C. Yuan and S. Thayumanavan, *Chem. Sci.*, 2013, **4**, 3654–3660.
28 L. Li and S. Thayumanavan, *Langmuir*, 2014, **30**, 12384–12390.
29 C. Yuan, K. Raghupathi, B. C. Popere, J. Ventura, L. Dai and S. Thayumanavan, *Chem. Sci.*, 2014, **5**, 229–234.
30 J. Ventura, S. J. Eron, D. C. González-Toro, K. Raghupathi, F. Wang, J. A. Hardy and S. Thayumanavan, *Biomacromolecules*, 2015, **16**, 3161–3171.
31 K. Dutta, D. Hu, B. Zhao, A. E. Ribbe, J. Zhuang and S. Thayumanavan, *J. Am. Chem. Soc.*, 2017, **139**, 5676–5679.
32 Z. Jiang, W. Cui, P. Prasad, M. A. Touve, N. C. Gianneschi, J. Mager and S. Thayumanavan, *Biomacromolecules*, 2018, **20**, 435–442.
33 E. F. Crownover, A. J. Convertine and P. S. Stayton, *Polym. Chem.*, 2011, **2**, 1499–1504.
34 K. C. R. Bahadur and P. Xu, *Adv. Mater.*, 2012, **24**, 6479–6483.
35 K. C. R. Bahadur, B. Thapa and P. Xu, *Mol. Pharmacol.*, 2012, **9**, 2719–2729.
36 K. C. R. Bahadur, V. Chandrashekaran, B. Cheng, H. Chen, M. M. O. Peña, J. Zhang, J. Montgomery and P. Xu, *Mol. Pharmacol.*, 2014, **11**, 1897–1905.
37 H. He, A. W. Cattran, T. Nguyen, A. L. Nieminen and P. Xu, *Biomaterials*, 2014, **35**, 9546–9553.
38 B. Cheng and P. Xu, *Toxins*, 2020, **12**, 582–594.

39 H. He, D. Altomare, U. Ozer, H. Xu, K. Creek, H. Chen and P. Xu, *Biomater. Sci.*, 2015, **4**, 115–120.
40 E. Markoutsa and P. Xu, *Mol. Pharmacol.*, 2017, **14**, 1591–1600.
41 H. He, E. Markoutsa, J. Li and P. Xu, *Acta Biomater.*, 2018, **68**, 113–124.
42 H. Asadi and S. Khoee, *Int. J. Pharmacol.*, 2016, **511**, 424–435.
43 A. W. Jackson and D. A. Fulton, *Macromolecules*, 2012, **45**, 2699–2708.
44 H. Palacio, F. Otálvaro, L. F. Giraldo, G. Ponchel and F. Segura-Sánchez, *Chem. Pharm. Bull.*, 2017, **65**, 1132–1143.
45 T. Cai, Y. Chen, Y. Wang, H. Wang, X. Liu, Q. Jin, S. Agarwal and J. Ji, *Polym. Chem.*, 2014, **5**, 4061–4068.
46 T. Cai, Y. Chen, Y. Wang, H. Wang, X. Liu, Q. Jin, S. Agarwal and J. Ji, *Macromol. Chem. Phys.*, 2014, **215**, 1848–1854.
47 H. S. Han, K. Y. Choi, H. Ko, J. Jeon, G. Saravanakumar, Y. D. Suh, D. S. Lee and J. H. Park, *J. Controlled Release*, 2015, **200**, 158–166.
48 J. G. Schellinger, J. A. Pahang, R. N. Johnson, D. S. H. Chu, D. L. Sellers, D. O. Maris, A. J. Convertine, P. S. Stayton, P. J. Horner and S. H. Pun, *Biomaterials*, 2013, **34**, 2318–2326.
49 Y. Sugawara, T. Tamaki, H. Ohashi and T. Yamaguchi, *Soft Matter*, 2013, **9**, 3331–3340.
50 H. Chen, H. Zou, H. J. Paholak, M. Ito, W. Qian, Y. Che and D. Sun, *Polym. Chem.*, 2014, **5**, 2768–2773.
51 Z. Song, Y. Xu, W. Yang, L. Cui, J. Zhang and J. Liu, *Eur. Polym. J.*, 2015, **69**, 559–572.
52 Y. Yang, Y. Li, Q. Lin, C. Bao and L. Zhu, *ACS Macro Lett.*, 2016, **5**, 301–305.
53 Z. Liu, Q. Lin, Y. Sun, T. Liu, C. Bao, F. Li and L. Zhu, *Adv. Mater.*, 2014, **26**, 3912–3917.
54 H. Peng, K. Rübsam, X. Huang, F. Jakob, M. Karperien, U. Schwaneberg and A. Pich, *Macromolecules*, 2016, **49**, 7141–7154.
55 X. Ji, J. Liu, L. Liu and H. Zhao, *Colloids Surf., B*, 2016, **148**, 41–48.
56 Y. Ju, C. Xing, D. Wu, Y. Wu, L. Wang and H. Zhao, *Chem. – Eur. J.*, 2017, **23**, 3366–3374.
57 L. Zhang, D. Zhang, Y. Yang and Y. Zhang, *Langmuir*, 2021, **37**, 3950–3959.
58 X. Ji, L. Liu and H. Zhao, *Polym. Chem.*, 2017, **8**, 2815–2823.
59 J. Lee, T. Zhao, D. J. Peeler, D. C. Lee, T. J. Pichon, D. Li, K. M. Weigandt, P. J. Horner, L. D. Pozzo, D. L. Sellers and S. H. Pun, *Soft Matter*, 2020, **16**, 3762–3768.
60 Z. Deng, J. Hu, S. Liu, Z. Deng, J. Hu and S. Liu, *Macromol. Rapid Commun.*, 2020, **41**, 1900531.
61 R. Zhang, T. Nie, Y. Fang, H. Huang and J. Wu, *Biomacromolecules*, 2022, **23**, 1–19.
62 A. Kock, K. Zuwala, A. A. A. Smith, P. Ruiz-Sanchis, B. M. Wohl, M. Tolstrup and A. N. Zelikin, *Chem Commun.*, 2014, **50**, 14498–14500.
63 A. A. A. Smith, B. M. Wohl, M. B. L. Kryger, N. Hedemann, C. Guerrero-Sanchez, A. Postma and A. N. Zelikin, *Adv. Healthcare Mater.*, 2014, **3**, 1404–1407.
64 C. F. Riber, A. A. A. Smith and A. N. Zelikin, *Adv. Healthcare Mater.*, 2015, **4**, 1887–1890.
65 P. Ruiz-Sanchis, B. M. Wohl, A. A. A. Smith, K. Zuwala, J. Melchjorsen, M. Tolstrup and A. N. Zelikin, *Adv. Healthcare Mater.*, 2015, **4**, 65–68.
66 K. Zuwala, A. A. A. Smith, M. Tolstrup and A. N. Zelikin, *Chem. Sci.*, 2016, **7**, 2353–2358.
67 M. Danial, A. H. F. Andersen, K. Zuwala, S. Cosson, C. F. Riber, A. A. A. Smith, M. Tolstrup, G. Moad, A. N. Zelikin and A. Postma, *Mol. Pharmacol.*, 2016, **13**, 2397–2410.
68 C. F. Riber, T. M. Hinton, P. Gajda, K. Zuwala, M. Tolstrup, C. Stewart and A. N. Zelikin, *Mol. Pharmacol.*, 2017, **14**, 234–241.
69 K. Zuwala, C. F. Riber, K. B. Løvschall, A. H. F. Andersen, L. Sørensen, P. Gajda, M. Tolstrup and A. N. Zelikin, *J. Controlled Release*, 2018, **275**, 53–66.
70 A. H. F. Andersen, C. F. Riber, K. Zuwala, M. Tolstrup, F. Dagnæs-Hansen, P. W. Denton and A. N. Zelikin, *ACS Macro Lett.*, 2018, **7**, 587–591.
71 C. K. Frich, F. Krüger, R. Walther, C. Domar, A. H. F. Andersen, A. Tvilum, F. Dagnæs-Hansen, P. W. Denton, M. Tolstrup, S. R. Paludan, J. Münch and A. N. Zelikin, *J. Controlled Release*, 2019, **294**, 298–310.
72 M. Danial, S. Telwatte, D. Tyssen, S. Cosson, G. Tachedjian, G. Moad and A. Postma, *Polym. Chem.*, 2016, **7**, 7477–7487.
73 Z.-H. Peng, Y. Xie, Y. Wang, J. Li and D. Oupický, *Mol. Pharmacol.*, 2017, **14**, 1395–1404.
74 W. J. Zhang, C. Y. Hong and C. Y. Pan, *Biomacromolecules*, 2016, **17**, 2992–2999.
75 P. Srikamut, T. Phakkeeree, F. Seidi, S. Iamsaard and D. Crespy, *ACS Appl. Polym. Mater.*, 2021, **3**, 5425–5433.
76 J. H. Ryu, R. Roy, J. Ventura and S. Thayumanavan, *Langmuir*, 2010, **26**, 7086–7092.
77 Q. Zhang, S. Aleksanian, S. M. Noh and J. K. Oh, *Polym. Chem.*, 2013, **4**, 351–359.
78 R. Baudry and D. C. Sherrington, *Macromolecules*, 2006, **39**, 1455–1460.
79 S. Durie, K. Jerabek, C. Mason and D. C. Sherrington, *Macromolecules*, 2002, **35**, 9665–9672.
80 M. Chisholm, N. Hudson, N. Kirtley, F. Vilela and D. C. Sherrington, *Macromolecules*, 2009, **42**, 7745–7752.
81 N. Sanson and J. Rieger, *Polym. Chem.*, 2010, **1**, 965–977.
82 N. V. Tsarevsky and K. Matyjaszewski, *Macromolecules*, 2005, **38**, 3087–3092.
83 H. Gao, N. V. Tsarevsky and K. Matyjaszewski, *Macromolecules*, 2005, **38**, 5995–6004.
84 N. V. Tsarevsky, K. Min, N. M. Jahed, H. Gao and K. Matyjaszewski, *ACS Symp. Ser.*, 2006, **939**, 184–200.
85 W. Li, K. Matyjaszewski, K. Albrecht and M. Möller, *Macromolecules*, 2009, **42**, 8228–8233.

86 W. Li, J. A. Yoon and K. Matyjaszewski, *J. Am. Chem. Soc.*, 2010, **132**, 7823–7825.
87 J. Kamada, K. Koynov, C. Corten, A. Juhari, J. A. Yoon, M. W. Urban, A. C. Balazs and K. Matyjaszewski, *Macromolecules*, 2010, **43**, 4133–4139.
88 M. Lamson, Y. Epshtein-Assor, M. S. Silverstein and K. Matyjaszewski, *Polymer*, 2013, **54**, 4480–4485.
89 V. Metri, A. Louhichi, J. Yan, G. P. Baeza, K. Matyjaszewski, D. Vlassopoulos and W. J. Briels, *Macromolecules*, 2018, **51**, 2872–2886.
90 Y. Wang and K. Matyjaszewski, *React. Funct. Polym.*, 2022, **170**, 105104.
91 Y. Li and S. P. Armes, *Macromolecules*, 2005, **38**, 8155–8162.
92 L. Wang, C. Li, A. J. Ryan and S. P. Armes, *Adv. Mater.*, 2006, **18**, 1566–1570.
93 C.-D. Vo, J. Rosselgong, S. P. Armes and N. C. Billingham, *Macromolecules*, 2007, **40**, 7119–7125.
94 Y. Li and S. P. Armes, *Macromolecules*, 2009, **42**, 939–945.
95 J. Rosselgong, S. P. Armes, W. Barton and D. Price, *Macromolecules*, 2009, **42**, 5919–5924.
96 J. Rosselgong, S. P. Armes, W. R. S. Barton and D. Price, *Macromolecules*, 2010, **43**, 2145–2156.
97 J. Rosselgong and S. P. Armes, *Macromolecules*, 2012, **45**, 2731–2737.
98 D. L. Popescu and N. V. Tsarevsky, *Aust. J. Chem.*, 2012, **65**, 28–34.
99 H. Tang and N. v. Tsarevsky, *J. Polym. Sci., Part A: Polym. Chem.*, 2016, **54**, 3683–3693.
100 N. V. Tsarevsky, J. Huang and K. Matyjaszewski, *J. Polym. Sci., Part A: Polym. Chem.*, 2021, **59**, 675–684.
101 Y. Gao, V. I. Böhmer, D. Zhou, T. Zhao, W. Wang and J. M. J. Paulusse, *J. Controlled Release*, 2016, **244**, 375–383.
102 T. Zhao, H. Zhang, B. Newland, A. Aied, D. Zhou and W. Wang, *Angew. Chem.*, 2014, **126**, 6209–6214.
103 B. Newland, A. Aied, A. v Pinoncely, Y. Zheng, T. Zhao, H. Zhang, R. Niemeier, E. Dowd, A. Pandit and W. Wang, *Nanoscale*, 2014, **6**, 7526–7533.
104 Y. J. Pan, Y. Y. Chen, D. R. Wang, C. Wei, J. Guo, D. R. Lu, C. C. Chu and C. C. Wang, *Biomaterials*, 2012, **33**, 6570–6579.
105 M. Zhang, S. Asghar, C. Tian, Z. Hu, Q. Ping, Z. Chen, F. Shao and Y. Xiao, *Carbohydr. Polym.*, 2021, **253**, 117194.
106 Y. Dai, Q. Li, S. Zhang, S. Shi, Y. Li, X. Zhao, L. Zhou, X. Wang, Y. Zhu and W. Li, *J. Drug Delivery Sci. Technol.*, 2021, **64**, 102650.
107 M. H. Loghmani, A. F. Shojaie and S. A. Hosseini, *J. Ind. Eng. Chem.*, 2021, **96**, 98–108.
108 Y. S. Lin, Y. L. Huang, W. F. Lee and C. H. Lin, *J. Chin. Chem. Soc.*, 2014, **61**, 945–952.
109 Q. B. Chen and Y. Z. You, *Chem. Lett.*, 2015, **44**, 677–679.
110 J. M. J. Paulusse, R. J. Amir, R. A. Evans and C. J. Hawker, *J. Am. Chem. Soc.*, 2009, **131**, 9805–9812.
111 L. P. D. Ratcliffe, C. Couchon, S. P. Armes and J. M. J. Paulusse, *Biomacromolecules*, 2016, **17**, 2277–2283.
112 J. Du, B. Choi, Y. Liu, A. Feng and S. H. Thang, *Polym. Chem.*, 2019, **10**, 1291–1298.
113 Y. Ma, X. Fu, Y. Shen, W. Fu and Z. Li, *Macromolecules*, 2014, **47**, 4684–4689.
114 W. Chen, Y. Zou, J. Jia, F. Meng, R. Cheng, C. Deng, J. Feijen and Z. Zhong, *Macromolecules*, 2013, **46**, 699–707.
115 S. Kim, K. I. Wittek and Y. Lee, *Chem. Sci.*, 2020, **11**, 4882–4886.
116 B. Yan, B. Liang, J. Hou, C. Wei, Y. Xiao, M. Lang and F. Huang, *Eur. Polym. J.*, 2020, **123**, 109452.
117 C. Wei, C. Lian, B. Yan, Y. Xiao, M. Lang and H. Liu, *Polym. Chem.*, 2020, **11**, 744–751.
118 C. Wei, Y. Zhang, B. Yan, Z. Du and M. Lang, *Chem. – Eur. J.*, 2018, **24**, 789–792.
119 V. B. Purohit, M. Pięta, J. Pietrasik and C. M. Plummer, *Polym. Chem.*, 2022, **13**, 4858–4878.
120 C. C. Chang and T. Emrick, *Macromolecules*, 2014, **47**, 1344–1350.
121 F. N. Behrendt and H. Schlaad, *Polym. Chem.*, 2017, **8**, 366–369.
122 F. N. Behrendt and H. Schlaad, *Macromol. Rapid Commun.*, 2018, **39**, 1700735.
123 F. N. Behrendt, A. Hess, M. Lehmann, B. Schmidt and H. Schlaad, *Polym. Chem.*, 2019, **10**, 1636–1641.
124 L. J. Reed and C. Niu, *J. Am. Chem. Soc.*, 1955, **77**, 416–419.
125 R. C. Thomas and L. J. Reed, *J. Am. Chem. Soc.*, 1956, **78**, 6148–6149.
126 J. A. Barltrop, P. M. Hayes and M. Calvin, *J. Am. Chem. Soc.*, 1954, **76**, 4348–4367.
127 Y. Ding and A. S. Hay, *Macromolecules*, 1996, **29**, 6386–6392.
128 Y. Ding and A. S. Hay, *Polymer*, 1997, **38**, 2239–2244.
129 Z. A. Liang, Y. Z. Meng, L. Li, X. S. Du and A. S. Hay, *Macromolecules*, 2004, **37**, 5837–5840.
130 Y. Z. Meng, Z. A. Liang, Y. X. Lu and A. S. Hay, *Polymer*, 2005, **46**, 11117–11124.
131 J. A. Chandrasiri and C. A. Wilkie, *Polym. Degrad. Stab.*, 1994, **46**, 275–284.
132 R. Arakawa, T. Watanabe, T. Fukuo and K. Endo, *J. Polym. Sci., Part A: Polym. Chem.*, 2000, **38**, 4403–4406.
133 K. Endo, T. Shiroi, N. Murata, G. Kojima and T. Yamanaka, *Macromolecules*, 2004, **37**, 3143–3150.
134 K. Endo, T. Shiroi and N. Murata, *Polym. J.*, 2005, **37**, 512–516.
135 H. Ishida, A. Kisanuki and K. Endo, *Polym. J.*, 2009, **41**, 110–117.
136 A. Kisanuki, Y. Kimpara, Y. Oikado, N. Kado, M. Matsumoto and K. Endo, *J. Polym. Sci., Part A: Polym. Chem.*, 2010, **48**, 5247–5253.
137 K. Endo and T. Yamanaka, *Macromolecules*, 2006, **39**, 4038–4043.
138 T. Yamanaka and K. Endo, *Polym. J.*, 2007, **39**, 1360–1364.
139 Y. Nambu, M. H. Acar, T. Suzuki and T. Endo, *Makromol. Chem.*, 1988, **189**, 495–500.
140 C.-Y. Shi, Q. Zhang, B.-S. Wang, M. Chen and D.-H. Qu, *ACS Appl. Mater. Interfaces*, 2021, **13**, 44860–44867.

141 C. Choi, J. L. Self, Y. Okayama, A. E. Levi, M. Gerst, J. C. Speros, C. J. Hawker, J. R. de Alaniz and C. M. Bates, *J. Am. Chem. Soc.*, 2021, **143**, 9866–9871.
142 C. Choi, Y. Okayama, P. T. Morris, L. L. Robinson, M. Gerst, J. C. Speros, C. J. Hawker, J. Read de Alaniz and C. M. Bates, *Adv. Funct. Mater.*, 2022, **32**, 2200883.
143 S. Maes, V. Scholiers and F. E. du Prez, *Macromol. Chem. Phys.*, 2021, 2100445.
144 S. Brännström, M. Johansson and E. Malmström, *Biomacromolecules*, 2019, **20**, 1308–1316.
145 T. Suzuki, Y. Nambu and T. Endo, *Macromolecules*, 1990, **75**, 1579–1582.
146 W. H. Stockmayer, R. O. Howard and J. T. Clarke, *J. Am. Chem. Soc.*, 1953, **75**, 1756–1757.
147 A. V. Tobolsky and B. Baysal, *J. Am. Chem. Soc.*, 1953, **7**, 1757.
148 H. Tang and N. V. Tsarevsky, *Polym. Chem.*, 2015, **6**, 6936–6945.
149 M. Raeisi and N. V. Tsarevsky, *J. Polym. Sci.*, 2021, **59**, 675–684.
150 E. K. Bang, G. Gasparini, G. Molinard, A. Roux, N. Sakai and S. Matile, *J. Am. Chem. Soc.*, 2013, **135**, 2088–2091.
151 G. Gasparini, E. K. Bang, G. Molinard, D. v. Tulumello, S. Ward, S. O. Kelley, A. Roux, N. Sakai and S. Matile, *J. Am. Chem. Soc.*, 2014, **136**, 6069–6074.
152 X. Zhang and R. M. Waymouth, *J. Am. Chem. Soc.*, 2017, **139**, 3822–3833.
153 Y. Liu, Y. Jia, Q. Wu and J. S. Moore, *J. Am. Chem. Soc.*, 2019, **141**, 17075–17080.
154 J. Lu, H. Wang, Z. Tian, Y. Hou and H. Lu, *J. Am. Chem. Soc.*, 2020, **142**, 1217–1221.
155 S. Huang, Y. Shen, H. K. Bisoyi, Y. Tao, Z. Liu, M. Wang, H. Yang and Q. Li, *J. Am. Chem. Soc.*, 2021, **143**, 12543–12551.
156 K. Margulis, X. Zhang, L. Joubert, K. Bruening, C. J. Tassone, R. N. Zare and R. M. Waymouth, *Angew. Chem.*, 2017, **129**, 16575–16580.
157 D. Witt, *Synthesis*, 2008, 2491–2509.
158 C. S. Sevier and C. A. Kaiser, *Nat. Rev. Mol. Cell Biol.*, 2002, **3**, 836–847.
159 M. W. Bullock, J. A. Brockman, E. L. Patterson, J. V. Pierce, M. H. von Saltza, F. Sanders and E. L. R. Stokstad, *J. Am. Chem. Soc.*, 1954, **76**, 1828–1832.
160 Q. F. Soper, W. E. Buting, J. E. Cochran Jr. and A. Pohland, *J. Am. Chem. Soc.*, 1954, **76**, 4109–4112.
161 E. L. Ruggles and R. J. Hondal, *Tetrahedron Lett.*, 2006, **47**, 4281–4284.
162 V. Kesavan, D. Bonnet-Delpon and J. P. Bégué, *Synthesis*, 2000, 223–225.
163 A. H. Nathan and M. T. Bogert, *J. Am. Chem. Soc.*, 1941, **63**, 2361–2366.
164 T. Lovato, V. Taresco, A. Alazzo, C. Sansone, S. Stolnik, C. Alexander and C. Conte, *J. Mater. Chem. B*, 2018, **6**, 6550–6558.
165 Y. S. Lin, Y. L. Huang, W. F. Lee and C. H. Lin, *J. Chin. Chem. Soc.*, 2014, **61**, 945–952.
166 C. Miao, F. Li, Y. Zuo, R. Wang and Y. Xiong, *RSC Adv.*, 2016, **6**, 3013–3019.
167 L. R. Jones, E. A. Goun, R. Shinde, J. B. Rothbard, C. H. Contag and P. A. Wender, *J. Am. Chem. Soc.*, 2006, **128**, 6526–6527.
168 F. Gauthier, A. Malher, J. J. Vasseur, C. Dupouy and F. Debart, *Eur. J. Org. Chem.*, 2019, 5636–5645.